Studies on the Glutathione *S*-Transferase Noppera-bo and its Role in Insect Ecdysteroid Biosynthesis

A Dissertation Submitted to
the Graduate School of Life and Environmental Sciences,
the University of Tsukuba
in Partial Fulfillment of the Requirements
for the Degree of Doctor of Philosophy in Science
(Doctoral Program in Biological Sciences)

Sora ENYA

Table of contents

Abstract

Steroid hormones regulate a number of biological events such as metabolism, homeostasis and development in many multicellular organisms. In insects, the timing of developmental transitions such as molting and metamorphosis is strictly determined by ecdysteroids including ecdysone that are synthesised from dietary cholesterol in the endocrine organ so-called the prothoracic gland (PG). Previous studies have identified and characterized several ecdysteroidogenic enzymes some of which are encoded by the Halloween genes. Here, I report a novel Halloween gene, *noppera-bo* (*nobo*), that encodes an epsilon class of the glutathione *S*-transferase (GST). *nobo* was identified as a gene that is predominantly expressed in the PG from the fruit fly *Drosophila melanogaster*. $nobo^{KO}$ mutants displayed embryonic lethality and a naked cuticle structure. These phenotypes are typical for Halloween mutants showing embryonic ecdysteroid deficiency. Additionally, the PG-specific *nobo* knock-down caused the developmental arrest phenotype with reduced 20-hydroxyecdysone (20E) titers. Importantly, both embryonic and larval phenotypes were rescued by the administration of 20E or cholesterol. Furthermore, abnormal cholesterol accumulation was observed in the PG of *nobo* knock-down animals. Considering that cholesterol is the most upstream material for ecdysteroid biosynthesis in the PG, my results indicate that *nobo* plays a crucial role in

regulating the behaviour of cholesterol in steroid biosynthesis in insects. I also conducted the phylogenetic analysis of GSTs, indicating that *nobo* is conserved in Diptera and Lepidoptera insects. *nobo-Bm,* orthologue from silkworm *Bombyx mori*, can be substituted for *Drosophila nobo (nobo-Dm)* in $nobo^{KO}$ mutants. These results strongly indicate that *nobo-Dm* and *nobo-Bm* are functionally orthologus. These findings are first reports that a GST controls cholesterol behavior to regulate steroid hormone biosynthesis.

Abbreviations

AEL: after egg laying

B. mori: Bombyx mori

C: cholesterol

CA: corpus allatum

CC: corpus cardiacum

cDNA: complementary DNA

CDS: coding sequence

dib: disembodied

D. melanogaster: Drosophila melanogaster

GSH: glutathione

GST: glutathione *S*-transferase

mm: millimeters

μm: micrometers

mRNA: messenger RNA

NPC: Niemann-Pick type C

nobo: noppera-bo

nvd: neverland

PG: prothoracic gland

ptth: prothoracicotropic hormone

RG: ring gland

RNAi: RNA interference

sad: shadow

shd: shade

spo: spook

spok: spookier

sro: shroud

tor: torso

20E: 20-hydroxyecdysone

7dC: 7-dehydrocholesterol

Introduction

Steroid hormone and insect development

Steroid hormones regulate a number of biological events such as metabolism, homeostasis, and development in many multicellular organisms (Mangelsdorf et al., 1995). During development, steroid hormones trigger developmental transitions from the juvenile stage to the adult stage. Examples of this are puberty in mammals and metamorphosis in insects (Chowen et al., 1996; Thummel, 2001). Defects in steroid hormone biosynthesis can cause developmental disorders and even lethality (Hu et al., 2002; Nebert et al., 2013; Niwa and Niwa, 2014). Thus, elucidating the mechanisms of steroid hormone biosynthesis is important for understanding development and physiology.

Ecdysteroids, the principal insect steroid hormones, including ecdysone and its active derivative form 20-hydroxyecdysone (20E), regulate embryogenesis and the timing of molting and metamorphosis (Gilbert et al., 2002; Riddiford, 1993) (Figure I). In a bioassay, ecsysone was linked to metamorphosis activity when it was isolated from the pupae of the silkworm *Bombyx mori* (Karlson, 1996). In postembryonic development, ecdysone is synthesized in the specialized endocrine

organ called the prothoracic gland (PG). The timing of ecdysone biosynthesis is controlled by several humoral factors such as prothoracicotropic hormone (PTTH) from the brain (McBrayer et al., 2007; Rewitz et al., 2009). In peripheral tissues, ecdysone is converted to 20E and then bound to the nuclear receptor composed of Ecdysone receptor (EcR) and Ultraspiracle (USP) (King-Jones and Thummel, 2005; Petryk et al., 2003). When 20E is bound to EcR/USP heterodimer, EcR/USP acts as a transcriptional factor and activates the transcription of downstream target genes known as ecdysone-inducible genes including *Broad-complex (BR-C), E74,* and *E75*. These ecdysone-inducible genes regulate further transcriptional cascades to initiate molting and metamorphosis (Thummel, 2001).

Ecdysone biosynthesis

Ecdysone is synthesized from dietary cholesterol or phytosterols. Unlike mammals, insects cannot synthesize *de novo* cholesterol from acetyl CoA. Therefore, insects must uptake sterols from food (Carvalho et al., 2010; Kurzchalia and Ward, 2003). In the intestine, phytosterols such as β-sitosterol are converted to cholesterol by specific enzymes (Awata et al., 1975; Ciufo et al., 2011; Fujimoto et al., 1980).

Cholesterol is bound to apolipoproteins to compose lipophorin, which is a spherical particle. It is thought that the lipophorin transport sterols from the intestine into the PG through hemolymph (Rodenburg and Van der Horst, 2005). Cholesterol in the PG is converted to ecdysone through several intermediates. The first conversion step is 7,8-dehydrogenation of cholesterol to produce 7-dehydrocholesterol (7dC). 7dC is then converted to 5β-ketodiol via steps that have not been identified – this process is known as a "Black Box" in the research community (Warren et al., 2009). The resulting 5β-ketodiol is sequentially hydroxylated at carbon 25, carbon 22, and carbon 2 to produce 5β-ketotriol, 2-deoxyecdysone, and ecdysone, respectively. Ecdysone is hydroxylated at carbon 20 to produce active derivative 20E in peripheral tissues (Gilbert et al., 2002; Niwa and Niwa, 2014) (Figure II).

Ecdysone biosynthesis enzymes

Enzymes involved in the conversion of cholesterol to 20E have been identified using molecular genetic analyses of *Drosophila melanogaster*. In 2000, *disembodied (dib)* mutant was characterized to show low ecdysteroid titer and the embryonic lethal phenotype with abnormal cuticle differentiation (Chávez et al., 2000). After

identifying *dib*, researchers focused on other mutants showing the same embryonic cuticle phenotype, including *shroud (sro)* (Niwa et al., 2010), *spook (spo)* (Namiki et al., 2005; Ono et al., 2006), *phantom (phm)* (Niwa et al., 2004; Warren et al., 2004), *shadow (sad)* (Jarcho et al., 2002), and *shade (shd)* (Petryk et al., 2003). They succeeded in identifying and characterizing ecdysone biosynthesis enzyme genes. With names referencing ghosts or spectres, these mutants (genes) are referred to as the Halloween mutants (genes) (Jarcho et al., 2002). From two transcriptome analyses in the PGs from *B. mori* and *D. melanogaster*, two ecdysone biosynthesis enzyme genes, *neverland (nvd)* (Yoshiyama et al., 2006) and *Cyp6t3* (Ou et al., 2011), have also been identified and characterized.

Biochemical analyses determined the conversion steps catalyzed by each ecdysone biosynthesis enzyme. *nvd* encodes the [2Fe-2S] Rieske oxygenese which catalyzes 7,8-dehydrogenation of cholesterol to produce 7dC (Yoshiyama-Yanagawa et al., 2011). *phm, dib, sad,* and *shd* encode cytochrome P450 monooxygenases and these proteins catalyze the hydroxylation at carbon 25, carbon 22, carbon 2, and carbon 20 of ecdysone intermediates, respectively (Jarcho et al., 2002; Niwa et al., 2004; Niwa et al., 2005; Petryk et al., 2003; Warren et al., 2004). It is still unknown what chemical reactions are catalyzed by the short-chain dehydrogenase/reductase Sro,

the cytochrome P450 monooxygenases CYP6T3, Spo, and its paralogue Spookier (Spok). However, there is some evidence to support the idea that these four enzymes are involved in the Black Box (Niwa et al., 2010; Ono et al., 2006; Ou et al., 2011).

Other genes related to ecdysone biosynthesis

Receptor tyrosine kinase encoded by *torso (tor)* receives a PTTH ligand and activates the expression of ecdysteroidogenic enzyme genes through RAS-MAPK signalling in the PG (Caldwell et al., 2005; Rewitz et al., 2009). Transforming growth factor-β (TGFβ) signalling components are also essential for the expression of certin ecdysteroidogenic genes including *nvd, dib,* and *spok* in the PG (Gibbens et al., 2011). *dnpc1a, dnpc2a, and dnpc2b, Drosophila* homologues of mammalian *Niemann-Pick type C (NPC)* genes, are involved in ecdysone biosynthesis via intracellular sterol trafficking and sterol homeostasis (Fluegel et al., 2006; Huang et al., 2005; Huang et al., 2007). Mutants of four genes, *dare* (Freeman et al., 1999), *ecdysoneless (ecd)* (Claudius et al., 2014; Gaziova et al., 2004), *molting defective (mld),* and *without children (woc)* (Warren et al., 2001; Wismar et al., 2000) exhibit low ecdysteroid titer and developmental defect phenotypes. While *ecd* is involved in

mRNA splicing of *spok* (Claudius et al., 2014), it is still unclear how the other three genes affect ecdysone biosynthesis.

Scope and short summary of this thesis

As described above, it has been reported that a number of genes acting in the PG encodes the *ptth* signalling components, sterol transporters, and ecdysteroidogenic enzymes. However, there are still uncertain mechanisms in ecdysone biosynthesis. For example, in the converting steps, intermediates in the Black Box have not been identified because the intermediates are thought to be chemically unstable. Furthermore, cholesterol uptake and trafficking in the PG is not well understood. It has been reported that a steroidogenic acute regulatory (StAR) protein has an essential role in steroidogenesis via regulating cholesterol translocation from the outer to inner mitochondrial membrane in mammals. Mutation in *StAR* protein gene causes steroid hormone deficiency (Stocco, 2001). *StAR* protein homologue gene *start1* has been identified in *D. melanogaster* and is highly expressed in the PG (Roth et al., 2004). However, *D. melanogaster start1* null mutants are developmentally normal, indicating that ecdysone biosynthesis is not disturbed in

mutants (Chen et al., 2009). Cholesterol homeostasis is controlled by sterol regulatory element binding proteins (SREBPs) that sense the amount of intracellular cholesterol and regulate the expression of cholesterol biosynthetic genes in mammals (Wang et al., 1994). Conversely, *Drosophila* SREBP proteins sense phosphatidylethanolamine instead of sterols as mammals and control gene expression for fatty acid synthesis (Dobrosotskaya et al., 2002; Seegmiller et al., 2002). Instead of mammalian SREBPs, cholesterol homeostasis is controlled by *Drosophila hormone receptor 96 (DHR96)* in the intestine of *Drosophila,* however, it has not been reported whether *DHR96* regulates cholesterol homeostasis in the PG to mediate ecdysone biosynthesis (Bujold et al., 2010; Horner et al., 2009; Sieber and Thummel, 2009).

With these facts in mind, I assumed that there are unidentified genes controlling ecdysteroid biosynthesis via catalyzing unknown conversion steps or cholesterol transport and homeostasis in the PG. To uncover the unidentified gene responsible for ecdysteroid biosynthesis, I tried to identify and characterize the novel gene involved in ecdysteroid biosynthesis.

Here, I report a novel ecdysteroidogenic gene in *D. melanogaster*, named *noppera-bo* (*nobo*), which encodes an epsilon class glutathione *S*-transferase (GST). *nobo* is predominantly expressed in ecdysone-producing organs. *nobo* and its orthologus genes are conserved in Diptera and Lepidoptera. *nobo* loss-of-function animals show a number of typical phenotypes caused by ecdysteroid deficiency. I demonstrate that *nobo* knock down causes cholesterol accumulation in the PG cells. I propose that *nobo* GST proteins are novel, indispensable regulators of ecdysteroid biosynthesis via regulating cholesterol behavior.

Results

Portions of data, figures and tables in this thesis have been previously published as: Enya S, Ameku T, Igarashi F, Iga M, Kataoka H, Shinoda T, Niwa R. (2014) A Halloween gene *noppera-bo* encodes a glutathione *S*-transferase essential for ecdysteroid biosynthesis via regulating the behaviour of cholesterol in *Drosophila*. Sci. Rep. 4: 6586. doi: 10.1038/srep06586.

CG4688/GSTe14 (*noppera-bo*) is expressed in the ecdysteroid biosynthetic organs.

From a microarray analysis using *D. melanogaster* to identify genes predominantly expressed in the ring gland (RG), a complex of endocrine organs composed of the PG, the corpus allatum (CA), and the corpus cardiacum (CC) (provided by Dr. Tetsuro Shinoda, unpublished data), I focused on *CG4688*, also known as *GSTe14,* which encodes an epsilon subclass glutathione *S*-transferase (Saisawang et al., 2012). A quantitative reverse-transcription (qRT-) PCR analysis revealed that *CG4688/GSTe14* was expressed in the RG at the third (final) instar larval stage and that the adult ovary sources ecdysone (Fig. 1a). *In situ* hybridization and immunohistochemical analyses demonstrated that *CG4688/GSTe14* was predominantly expressed in the PG cells at the third instar larval stages (Fig. 1b, c), as well as in ovarian follicle cells from adult (Fig. 1d, e). The RG is composed of the PG, the CA, and the CC. *CG4688/GSTe14* was exclusively expressed in the PG but

not in the CA or the CC (Fig. 1b', c'). It has been reported that expression of most ecdysteroidogenic enzyme genes in the PG are positively regulated by prothoracicotropic hormone (PTTH) and its receptor Torso (McBrayer et al., 2007; Niwa et al., 2005; Niwa et al., 2010; Rewitz et al., 2009; Yamanaka et al., 2007; Yamanaka et al., 2013). I found that the mRNA level of *CG4688/GSTe14* was also significantly decreased in the third instar larvae of *ptth* neuron-ablated and *torso* RNA interference (RNAi) animals compared to that of controls (Fig. 1f).

Temporal expression pattern of *CG4688/GSTe14* is collated with ecdysteroid titer in embryonic stage

In *D. melanogaster* the zygotic expression of the Halloween genes is essential for ecdysteroid biosynthesis prior to formation of the PG in the early embryonic stage (Chávez et al., 2000; Niwa et al., 2010; Ono et al., 2006). The temporal embryonic expression of *CG4688/GSTe14* correlated well with a change in the embryonic ecdysteroid titer (Fig. 2a) (Maróy et al., 1988). While no or little maternal *CG4688/GSTe14* mRNA was detected, embryonic *CG4688/GSTe14* expression was a maximum at 2-6 hours after egg laying (AEL) (Fig. 2a), which roughly corresponds to embryonic stages 5-10 (Fig. 2b-e). *CG4688/GSTe14* expression decreased after 6

hours AEL (Fig. 2a). It is important to note that the temporal expression pattern of *CG4688/GSTe14* resembles that of *shroud (sro)* (Fig. 2a), which has already been previously described (Niwa et al., 2010). I also performed *in situ* RNA hybridization analysis to examine the expression pattern of *CG4688/GSTe14* during embryogenesis. *CG4688/GSTe14* mRNA was detected in the blastoderm embryo in stage 5 (Fig. 2b). After cellularization, *CG4688/GSTe14* expression was observed almost ubiquitously in the epidermal cells (Fig. 2c-e). In the germband elongation stage (stage 11), expression level of *CG4688/GSTe14* increased in the amnioserosa (Fig. 2f). At stage 16 and later, *CG4688/GSTe14* expression was detected in the PG cells (Fig. 2g). Previous studies demonstrated that certain Halloween genes are also expressed in the epidermal cells, the amnioserosa, and the PG (Niwa et al., 2004; Ono et al., 2006; Warren et al., 2004). All of these results together indicate that *CG4688/GSTe14* expression pattern is strongly correlated with ecdysteroid biosynthesis. Hereafter, I will refer to *CG4688/GSTe14* as *noppera-bo* (*nobo*), for reasons to be explained later.

Noppera-bo is a novel Halloween gene

With identification of *noppera-bo (nobo)*, I subsequently focused on elucidating its

functional importance *in vivo*. Previous studies have shown that six ecdysteroidogenic enzyme genes, *spo* (Namiki et al., 2005; Ono et al., 2006), *sro* (Niwa et al., 2010), *phm* (Niwa et al., 2004; Warren et al., 2004), *dib* (Chávez et al., 2000), *sad* (Jarcho et al., 2002), and *shd* (Petryk et al., 2003) belong to the Halloween genes, which were originally identified in Nüsslein-Volhard and Wieschaus' large saturated mutant screen and characterised as the embryonic lethality with undifferentiated cuticle structure (Jürgens et al., 1984; Nüsslein-Volhard et al., 1984; Wieschaus et al., 1984). While *nobo* is located at the 49F12 cytological position of the right arm of the 2nd chromosome, typical Halloween mutants were not in the vicinity of *nobo* in the previous screen (Nüsslein-Volhard et al., 1984).

I created a null mutant of *nobo* by conventional knock-out technique (Rong and Golic, 2000). In my *nobo* knock-out allele ($nobo^{KO}$), an almost-open reading frame of *nobo* was replaced with a *mini-white* marker gene (Fig. 3a). Homozygous mutants of $nobo^{KO}$ showed the embryonic lethal phenotype and, like other Halloween mutants, showed undifferentiated cuticle structure (Fig. 3b, c). I also found that homozygous mutants of $nobo^{KO}$ displayed abnormal morphologies that involve head involution defective, dorsal open, and abnormal gut looping (Fig. 4a-d).

Moreover, the epidermal expression of both *IMP-E1* and *IMP-L1*, which are ecdysteroid-inducible genes, was greatly reduced or absent in homozygous mutants of $nobo^{KO}$ (Fig. 4a-d). The reduced expression of ecdysone-inducible genes indicates that $nobo^{KO}$ mutants cause ecdysone deficiency. These phenotypes very closely resemble the features of Halloween mutants (Chávez et al., 2000). I also confirmed that the lethality and phenotype of $nobo^{KO}$ mutants was caused solely by the loss of *nobo* function, as shown by the result that lethality was completely rescued by exogenous *nobo* expression driven by *phm-GAL4#22* using the GAL4/UAS system (Brand and Perrimon, 1993) (Fig.5 and Table 1).

I next determined whether the lethality of the $nobo^{KO}$ mutant could be rescued by administration of 20E through embryogenesis. Without 20E treatment, no $nobo^{KO}$ homozygous embryos developed into first instar larvae (Table 2). On the other hand, with 100 μM 20E administration, some $nobo^{KO}$ homozygous embryos hatched into first instar larvae (Table 2), whereas the rescued $nobo^{KO}$ mutant larvae died at the first instar larvae and did not grow into the second instar stage on standard cornmeal food (100%; N=46). These results indicate that *nobo* is required for embryonic ecdysteroid biosynthesis and can indeed be classified as a Halloween gene. On the basis of the Halloween-class naked cuticle phenotype, I named

CG4688/GSTe14 '*noppera-bo*' after a legendary Japanese faceless ghost.

Noppera-bo is an essential gene for ecdysteroid biosynthesis during larval development

To investigate the importance of *nobo* during larval development, I examined the phenotypes of overexpression and knockdown using the GAL4/UAS system (Brand and Perrimon, 1993). In a wild-type background, the overexpression of *nobo* using ubiquitous *tub-GAL4* and the PG specific *phm-GAL4 #22* driver lines had no phenotype on development (data not shown). For *nobo* knockdown, I performed transgenic RNAi experiments (Kennerdell and Carthew, 2000) using transgenic lines carrying an inverted repeat construct corresponding to the *nobo* mRNA fused to UAS promoter region (*UAS-nobo-IR*). When the *UAS-nobo-IR* was driven by *phm-GAL4#22,* the *nobo* RNAi animals showed larval lethality. Larval lethality was observed with two independent *UAS-nobo-IR* constructs (#40316 and #101884 provided from the Vienna *Drosophila* RNAi Center), each of which targeted a different region of the *nobo* mRNA. Larval lethality was also observed using other GAL4 lines that are expressed in the PG cells (Table 3). I therefore conclude that *nobo* has an essential role in the PG during larval stages. Hereafter, I will refer to

animals in which the *nobo* RNAi was driven by *phm-GAL4#22* with *UAS-nobo-IR* (*#40316*) as '*nobo* RNAi animals'.

The lethal phase for *nobo* RNAi animals was examined in more detail. In *nobo* RNAi animals, *nobo* mRNA levels were reduced to 1% of control animals at the first instar stage (Fig. 6a). *nobo* RNAi animals hatched normally and showed no apparent morphological or behavioral defects at 24 hours after egg laying (AEL), i.e., until the first instar larval stage (Fig. 6b, c). However, at ~48 hours AEL, *nobo* RNAi animals exhibited apparent growth defects compared to control animals (Fig. 6b-d). At 72 hours AEL, as ~50% of control animals grew to the third instar larval stage (Fig. 6b, e), ~80% of *nobo* RNAi animals remained in the second instar larvae (Fig. 6c, e). At 144 hours AEL, ~90% of control animals became pupae (Fig. 6b, f), however, *nobo* RNAi animals were in the second instar stage and gradually died (Fig. 6c, f). At 240 hours AEL, ~80% of control animals became adults (Fig. 6b). At this time, ~90% of *nobo* RNAi animals had already died, and the few larvae that were still alive were arrested at the second instar larval stage (Fig. 6c). I also found that the larval arrest phenotype and lethality of *nobo* RNAi animals was due to ecdysteroid deficiency. I first examined ecdysteroid titer in the second instar larvae (60 hours AEL) of control and *nobo* RNAi animals by mass-spectrometric analysis.

In the control larvae, 1.55 ± 0.27 pg of 20E/mg of wet weight (mean ± s.e.m., N=5) was detected. In contrast, ecdysteroid titer in *nobo* RNAi animals (N=5) was under the quantifiable limit under identical experimental conditions (see Methods). These results suggest that *nobo* RNAi caused ecdysteroid biosynthesis defects during larval stages (Mass-spectrometric analysis was carried out by Dr. Masatoshi Iga). Moreover, I tested whether the *nobo* RNAi phenotype was rescued by administration of 20E. When *nobo* RNAi animals were fed 20E containing food from the first instar larvae, they grew to the later larval, pupal, and even adult stages (Fig. 8a, inset). These results indicate that, in addition to embryogenesis, *nobo* is also essential for larval development via regulating ecdysteroid biosynthesis.

Administration of cholesterol rescues *noppera-bo* loss-of-function phenotypes.

To determine which step(s) of ecdysteroid biosynthesis is affected by the loss of *nobo* function, I performed feeding experiments using several intermediates of 20E. If Nobo is involved in a certain ecdysteroid biosynthesis step, I hypothesized that the larval arrest phenotype of *nobo* RNAi would be rescued by an administration of intermediate(s) downstream of the biosynthesis step. In previous studies, the same logic has been applied to confirm the conversion steps of some ecdysteroidogenic

enzymes, such as Sro (Niwa et al., 2010) and Nvd (Yoshiyama et al., 2006). Intriguingly, I found that embryonic lethality of *nobo*^{KO} mutants was almost completely rescued when their mothers were fed yeast paste containing 0.5% (w/w) cholesterol or 7-dehydrocholesterol (7dC) (Table 4). I confirmed the homozygosity of the rescued *nobo*^{KO} first instar larvae by genomic PCR (Fig. 7). Similarly, when the *nobo* RNAi larvae were fed food containing cholesterol or 7dC, they molted normally and grew into the adult stage (Fig. 8a). Considering the conventional view that cholesterol is the most upstream material of ecdysteroids in the PG (Gilbert et al., 2002; Niwa and Niwa, 2011), these results suggest that Nobo may not be involved in the conversion step of identified ecdysteroid intermediates; but rather it may play a role in metabolism and/or transport of cholesterol in the PG.

I also tested the developmental progression of the homozygous *nobo*^{KO} first instar larvae, which were derived by maternal application of cholesterol as described above. On a standard cornmeal food, all of the rescued *nobo*^{KO} homozygous larvae showed a developmental arrest phenotype at the first or second instar larval stage (Table 5). This larval arrest phenotype was due to ecdysteroid deficiency because the rescued *nobo*^{KO} homozygous first instar larvae grew to the third instar larval stage on a diet supplemented with 20E (Table 5). In contrast to

the RNAi animals, the larval arrest phenotype of the *nobo*^{KO} larvae was not rescued when they were fed cholesterol- or 7dC-supplemented food (Table 5). These results suggest that the PG cells from the rescued *nobo*^{KO} larvae cannot utilize cholesterol for ecdysteroid biosynthesis during larval development, whereas the PG cells from *nobo* RNAi, which are partial *nobo* loss-of-function, can. This point is argued in the Discussion section below.

Noppera-bo plays a crucial role in cholesterol transport and/or metabolism

I tested whether cholesterol in the PG cells was affected in *nobo* RNAi animals. A mass-spectrometric study revealed that cholesterol accumulated significantly in the PG from *nobo* RNAi animals compared to that from control animals (Fig. 8b). There were no statistically significant differences in the amounts of other plant and fungal sterols, such as β-sitosterol, ergosterol and campesterol, contained in the standard cornmeal food provided between control and *nobo* RNAi RG cells (Fig. 8b). 7dC was not detected in either control or RNAi RG cells. To further confirm cholesterol accumulation in the RG, the RGs from control and *nobo* RNAi larvae were dissected and incubated in culture medium with 22-NBD-cholesterol, a fluorescent analogue of cholesterol (Scheidt et al., 2003). There were significantly increased fluorescence

signals in the PG cells from *nobo* RNAi larvae compared to that of control animals (Fig. 8c, d). These results suggest that Nobo is essential for appropriate metabolism and/or transport of cholesterol for ecdysteroid biosynthesis.

A subfamily of *noppera-bo* GST genes is well conserved in diptera and lepidoptera

As classical phase II detoxification enzymes, GSTs are thought to have rapidly evolved in response to various toxins and insecticides; thus, each insect genome encodes multiple GST genes (Friedman, 2011). *nobo* is found in the genomes of not only *D. melanogaster* but also other *Drosophila* species (Chanut-Delalande et al., 2014; Clark et al., 2007). I tested the evolutionarily conservation of *nobo* using the phylogenetic analysis among Nobo and the other 277 GST proteins from 11 insects, the nematode *Caenorhabditis elegans,* and *Homo sapiens* (Fig. 9a). Nobo belongs to the epsilon subclass, one of the six subclasses of insect cytosolic GSTs (Saisawang et al., 2012). In the epsilon cluster, phylogenetic analysis revealed that *D. melanogaster* Nobo is included in an evolutionarily conserved subclade, which also includes GSTs from dipteran species other than Drosophilidae species, such as the mosquitoes *Aedes aegypti*, *Anopheles gambiae*, and *Culex quinquefasciatus*, as well as lepidopteran species such as the silkworm *Bombyx mori* and the monarch

butterfly *Danaus plexippus* (Fig. 9a, b). The orthologous relationships between *A. gambiae*, *B. mori,* and *D. melanogaster* are consistent with previous reports (Ayres et al., 2011; Yu et al., 2008). This conservation feature is in contrast to many other GSTs, which are duplicated within its species (Fig. 9a). In contrast, no clear orthologs of *nobo* were found in insects other than dipteran and lepidopteran species. These results suggest that *nobo* is evolutionarily conserved exclusively in Diptera and Lepidoptera.

According to the current GST nomenclature system, the orthologues of *nobo* from *D. melanogaster*, *A. gambiae,* and *B. mori* are named GSTe14 (Saisawang et al., 2012), GSTe8 (Ayres et al., 2011), and GSTe7 (Yu et al., 2008), respectively. As will be described in further detail later, I succeeded in demonstrating that *B. mori GSTe7* was functionally orthologous to *D. melanogaster nobo*. To avoid further confusing numberings that represent the same functional orthologues among insect species, I would like to propose a unique subfamily name, *noppera-bo* (*nobo*), for these orthologues. Hereafter in this thesis, I will refer to *B. mori GSTe7* as *nobo-Bm*.

For the phylogenetic analysis, I also included human GSTA subclass members because previous studies have reported that certain GSTA proteins are involved in steroidogenesis in mammals (Fedulova et al., 2010; Johansson and

Mannervik, 2001; Raffalli-Mathieu et al., 2008; Tars et al., 2010). I found that the mammalian GSTA proteins were clustered in a clade completely different from the Nobo subclade (Fig. 9a).

Noppera-bo GSTs play a conserved and specific role in insects

To examine whether other insect orthologues of *nobo* also play conserved roles in ecdysteroid biosynthesis, I tested whether *nobo-Bm* can compensate for *D. melanogaster nobo* loss-of-function during development. Indeed, the *phm-GAL4*-driven expression of *nobo-Bm* allowed both $nobo^{KO}$ homozygous mutants and *nobo* RNAi animals to complete development and grow to adult stages (Tables 1 and 6). These results suggest that *nobo* genes are truly functionally orthologous between Diptera and Lepidoptera. These data also confirm that the effect of RNAi was specific to *nobo* and was not an off-target effect.

I further utilized the overexpression system to examine the functional specificity of *nobo* among other GST genes. A protein BLAST search indicated that the Nobo protein sequence is most similar to two epsilon-class GSTs in *D. melanogaster*, GSTe4, and GSTe12. However, neither *GSTe4* nor *GSTe12* overexpression was able to rescue the lethality of *nobo* loss-of-function animals

(Tables 1 and 6). I also obtained previously reported transgenic lines to overexpress other *D. melanogaster* GST genes, including *sepia*, *CG6662*, *CG6673A,* and *CG6673B* (Kim et al., 2006), known as *GSTO4, GSTO1, GSTO2A,* and *GSTO2B,* respectively (Saisawang et al., 2012). In particular, *sepia* is known to be involved in eye pigment synthesis and *CG6673A* is liked to a neurodegeneration process. Their substrates have already been identified (Kim et al., 2006; Kim et al., 2012). However, the overexpression of none of these genes rescued lethality of *nobo* loss-of-function animals (Tables 1 and 6). These results support the notion that *nobo* GSTs plays a unique role in controlling ecdysteroid biosynthesis.

Discussion

Noppera-bo (*nobo*)/*GSTe14* is a novel ecdysteroidogenic gene

In this study I identified *noppera-bo* (*nobo*)/*GSTe14,* a gene encoding epsilon subfamily of Glutathione S-transferase (GST), as a new component of the ecdysteroid biosynthetic pathway. All of my results indicate that the Nobo protein plays a crucial role in ecdysteroid biosynthesis in *Drosophila melanogaster*. Both the expression profile data and genetic analysis strongly indicate that *nobo* has an essential role for ecdysone biosynthesis in the embryonic and larval stages of *Drosophila melanogaster*. The expression profile in this study demonstrated that *nobo* is expressed in embryonic tissues including the epidermis and the amnioserosa, the larval prothoracic gland (PG), and the adult ovary. This expression pattern strongly correlates with ecdysone biosynthesis. $nobo^{KO}$ mutant embryos showed lethality with the morphogenetic abnormalities that have previously been observed in Halloween mutants. This lethality was rescued by administration of 20-hydroxyecdysone (20E). The PG-specific *nobo* RNAi animals displayed developmental arrest phenotype with reduced 20E titer. This arrest phenotype was completely rescued by administration of 20E. Interestingly, the developmental phenotypes in loss of *nobo* function animals were rescued not only by administration of 20E, but also cholesterol. Cholesterol is the most upstream

material of ecdysteroid in the PG, so it seems probable that Nobo does not catalyze a chemical reaction of ecdysone biosynthesis but may control cholesterol behavior for ecdysone biosynthesis. It is notable that the *GSTe14* function in ecdysone biosynthesis has been independently demonstrated by other researchers (Chanut-Delalande et al., 2014). To my knowledge, however, this is the first study reporting that GST regulates development and cholesterol behavior.

Nobo is involved in ecdysone biosynthesis via regulating cholesterol behavior

Because insects cannot synthesize cholesterol *de novo*, it is necessary for them to uptake cholesterol or phytosterol from their diets (Clark and Bloch, 1959). The data provided in this study demonstrates that abnormal accumulation of cholesterol occurred in the PG from *nobo* RNAi larvae. Additionally, in the tissue culture experiment using a NBD-cholesterol (fluorescent analogue of cholesterol), fluorescence levels of NBD-cholesterol were increased in the PG from *nobo* RNAi larvae. These results raise two possibilities in the PG of wild type larvae: (1) Nobo inhibits uptake cholesterol from hemolymph into the PG and thus acts as a negative regulator for ecdysone biosynthesis; or (2) Nobo is essential for cholesterol utilization via the proper intracellular trafficking of cholesterol in the PG and thus

acts as a positive regulator for ecdysone biosynthesis. Genetic analyses favored that the latter possibility because *nobo* mutants and *nobo* RNAi larvae showed ecdysone deficiency phenotype and overexpression of *nobo* had no effect on development in wild type. Therefore I conclude that Nobo is a positive regulator for ecdysone biosynthesis (Figure 10).

Related to this point, *nobo* RNAi phenotypes resemble a mutant of *dnpc1a,* which is the *Drosophila* homologue of the mammalian *Niemann-Pick type C1 (NPC1)* that regulates cholesterol trafficking in steroidogenic organs (Rosenbaum and Maxfield, 2011). *dnpc1a* mutants exhibit larval developmental arrest phenotype, ecdysone deficiency, and abnormal sterol accumulation in the PG. The larval arrest phenotype of the *dnpc1a* mutant is also rescued by high cholesterol or 7dC diets (Fluegel et al., 2006; Huang et al., 2005). This consistency also supports the hypothesis that Nobo controls ecdysone biosynthesis by regulating the behaviour of intracellular cholesterol in the PG.

This study revealed that embryonic lethality of the $nobo^{KO}$ homozygous mutant can be rescued by maternal supplement of cholesterol; however, larval arrest phenotype of the rescued $nobo^{KO}$ homozygote was not rescued by cholesterol administration. A possible explanation for these phenotypic differences is as follows. In oogenesis,

mother flies load maternal factors essential for embryogenesis, including maternal mRNAs and nutrients, into eggs. Under normal food conditions for the mother flies, cholesterol is loaded into the yolk or cytoplasm of the eggs. This cholesterol needs to be transported to the endoplasmic reticulum (ER) or microsomes by Nobo to incorporate cholesterol into the ecdysone biosynthetic pathway because 7,8 dehydrogenation of cholesterol - the first conversion step of ecdysone biosynthesis - occurs in ER or microsomes (Grieneisen et al., 1993; Yoshiyama-Yanagawa et al., 2011). When mother flies are fed a high cholesterol diet, excessive cholesterol is loaded into not only the yolk and cytoplasm but also the ER and microsomes. Cholesterol accumulation in the ER or microsomes is sufficient to produce ecdysone for embryogenesis even if Nobo function is disrupted. In contrast, larval PG should uptake cholesterol from hemolymph for larval ecdysone biosynthesis. In this process Nobo is necessary to transport cholesterol into the ER or a microsome. so $nobo^{KO}$ mutant larvae are not rescued by oral cholesterol administration.

Another question is why the phenotype of *nobo* RNAi larvae can be rescued by oral cholesterol administration even though excessive cholesterol is accumulated in the PG. One possibility is that a most cholesterol is unusually accumulated as an unavailable form for ecdysone biosynthesis in the PG of *nobo* RNAi larvae under

normal diet conditions. On the other hand, if a large amount of cholesterol is supplied in a diet, some cholesterol will be delivered into the ecdysone biosynthesis pathway even though Nobo function is disrupted. These phenotypes were observed in *dnpc1a* mutants (Huang et al., 2005). In both cases, the mechanism causing cholesterol accumulation in the PG is unclear, so it is important to identify the pathway affected by Nobo.

Molecular function of Nobo as GST

It has been reported that GST proteins conjugate the reduced form of glutathione (GSH) to various substrates (Board and Menon, 2013; Hayes and Pulford, 1995). Generally, GSTs are known as Phase II metabolic enzymes that catalyse the conjugation of GSH to xenobiotic substrates, including pollutants and drugs, for detoxification in eukaryotes because GSH-conjugated substrates become more hydrophilic and are usually excreted from cells through ABC transporters (Frova, 2006; Tew and Townsend, 2012). In insects, GSTs are also essential enzymes for detoxifying endogenous and exogenous compounds such as insecticides. In particular, interest in insect GSTs primarily focuses on their role in insecticide resistance (Enayati et al., 2005) and phytochemical detoxification (Shabab et al.,

2014; Sun et al., 2013). Other studies report that certain GSTs are involved in the regulation of cellular signal transduction cascades and the production of essential metabolites in insects (Kim et al., 2006; Kim et al., 2012) and vertebrates (Laborde, 2010; Tew et al., 2011). Combining such findings with those of this study, it is clear that Nobo has an essential role in regulating endogenous, rather than exogenous, molecules.

It is possible that Nobo conjugates GSH directly to small bioactive compound(s), such as cholesterol and/or other sterols, to become more hydrophilic. In the plant *Arabidopsis thaliana* 12-oxo-phytodienoic acid (OPDA), the precursor of jasmonic acid, is conjugated with GSH, which is an important process for the transportation of OPDA into the vacuole (Ohkama-Ohtsu et al., 2011). Like the OPDA-GSH compound, the sterol-GSH compound may be essential for proper sterol trafficking in the PG.

Another possibility is that Nobo might conjugate GSH into a protein that has an essential role in regulating the cholesterol behavior in the PG. In mammals several GSTs conjugate GST to endogenous proteins to modulate certain functions (Tew et al., 2011). It is possible that Nobo conjugates GSH to a protein that regulates cholesterol behavior.

It has been also reported that certain GSTs act as transporters or carriers for small molecules with the GSH conjugation activity in an independent manner. In *A. thaliana,* Transparent Testa 19 (TT19), one of the *Arabidopsis* GSTs, is bound with anthocyanins, which is one of the pigments in plants. TT19 transports anthocyanins from cytoplasm to tonoplasts (Sun et al., 2012). With this in mind, it may be true that *nobo* directly binds with cholesterol or other sterols to transport them in the PG. To investigate these hypotheses, it is necessary to identify the target or the binding partner of Nobo. The only hint regarding the substrate(s) of Nobo revealed by transgenic rescue experiments using several types of GST proteins is that Nobo most likely has relatively narrow substrate specificity.

Steroidogenic GSTs in mammals

Previous studies have demonstrated that human GST A3-3 and its counterparts in other mammals are involved in mammalian steroid hormone biosynthesis (Fedulova et al., 2010; Johansson and Mannervik, 2001; Raffalli-Mathieu et al., 2008; Tars et al., 2010). Human GST A3-3 is selectively expressed in steroidogenic organs and catalyzes the isomerisation of the Δ^5-ketosteroid precursor to produce progesterone and testosterone (Johansson and Mannervik, 2001). In conjunction

with the studies in mammals, my study raises an interesting possibility that, similar to the families of cytochrome P450s and short-chain dehydrogenase/reductases (Gilbert, 2004; Niwa et al., 2010), the GST family is also involved in steroid hormone biosynthesis across animal phyla.

On the other hand, even though GSTA 3-3 and Nobo are involved in sterodogenesis, their molecular functions are quite different. It has not been reported that mammalian GST controls cholesterol trafficking and insect GST catalyzes a conversion step of steroid biosynthesis. Additionally, as described in the introduction, it has been known in mammals that cholesterol trafficking is regulated by proteins NPC1 and StAR protein in steroidogenic organs (Rosenbaum and Maxfield, 2011; Stocco, 2001). In *Drosophila*, *dnpc1a* is also involved in cholesterol trafficking but *start1,* the StAR homologue in *Drosophila*, may not be involved in (Chen et al., 2009; Huang et al., 2005; Roth et al., 2004). Considering both the mammal and insect cases together, certain components for cholesterol trafficking seem to be conserved while others are not.

Conservation of Nobo subfamily

The phylogenetic analysis performed in this study indicates that the *nobo* subfamily

of GST proteins is well conserved in Diptera and Lepidoptera. It is also demonstrated that the *in vivo* function of *D. melanogaster nobo* can be replaced with *B. mori nobo* (*nobo-Bm*), suggesting a functional orthologous relationship of *nobo* between Diptera and Lepidoptera. It can be reasoned that the ancestor GST gene of the *nobo* subfamily was acquired in an ancestor of Diptera and Lepidoptera. This might explain why I was unable to find any clear orthologues of *nobo* in any other insect taxons (Fig. 9a).

Because the GST family has great intra- and inter-species functional and structural diversity, it is possible that the simple BLAST search strategy and neighbour-joining method employed in this study failed to discover the Nobo orthologues in other insect species. Another possible explanation is that ecdysteroid biosynthesis is differently regulated among different insect species. Curiously, the essential ecdysteroidogenic enzyme genes *spookier* and *Cyp6t3* have so far only been found in the genomes of Drosophilidae (Ono et al., 2006; Ou et al., 2011). In the future, it would be very interesting to study not only the evolutionarily conservation of ecdysteroidogenic enzymes in arthropods (Rewitz et al., 2006; Rewitz et al., 2007), but also the specific molecular mechanisms of ecdysteroid biosynthesis in certain insects.

Material and Methods

Fly strains

Drosophila melanogaster flies were reared on standard agar-cornmeal medium at 25°C under a 12 h/12 h light/dark cycle. Oregon R was used as the wild-type strain for the *in situ* RNA hybridization and immunohistochemistry, as shown in Fig. 1. *white*^{1118} (*w*^{1118}) was used as the wild-type (control) strain for all genetic experiments. The *UAS-nobo-IR* (stock numbers #40316 and #101884) and *UAS-torso-IR* (stock number #101154) strains were obtained from the Vienna *Drosophila* RNAi Center. *yw; P{CaryP}attP40* (Markstein et al., 2008) was obtained from BestGene, Inc. *ptth-GAL4;UAS-grim*, in which the *ptth* gene-expressing neurons were ablated (McBrayer et al., 2007), *phm-GAL4#22* (McBrayer et al., 2007; Ou et al., 2011), and *UAS-dicer2* were kindly gifted by M. B. O'Connor (University of Minnesota, USA). *UAS-sepia*, *UAS-CG6673A*, *UAS-CG6673B,* and *UAS-CG6662* (Kim et al., 2006) were kind gifts from J. Yim (National University Seoul, Korea). *yw; P{70FLP}23 P{70I-SceI}4A/TM6* (Rong and Golic, 2000) and *w; P{70FLP}10* (Rong and Golic, 2000) were obtained from the Bloomington Drosophila Stock Center. *2-286-GAL4* (Timmons et al., 1997), *Act5c-GAL4* (Namiki et al., 2005), *Akh-GAL4* (Lee and Park, 2004), *Aug21-GAL4* (Siegmund and Korge, 2001), *daughterless-GAL4* (Wodarz et al., 1995), *elav-GAL4* (Luo et al., 1994), *NPC1b-GAL4* (Voght et al., 2007), *phm-GAL4*

(w1) (Ono et al., 2006), and *tub-GAL4* (Lee and Luo, 1999) lines maintained in the Niwa laboratory were used in the tissue specific RNAi experiments.

Quantitative reverse transcription (qRT)-PCR

Total RNA was isolated using RNAiso Plus reagent (TaKaRa). Genomic DNA was digested using Recombinant DNaseI (TaKaRa). cDNA was synthesised using the ReverTra Ace qRT RT Kit (TOYOBO). qRT-PCR was performed using THUNDERBIRD SYBR qPCR Mix (TOYOBO) with a Thermal Cycler Dice TP800 system (TaKaRa). Serial dilutions of a plasmid containing the ORF of each gene were used as a standard. The expression levels were normalised to *rp49* in the same sample. The primers for quantifying *D. melanogaster nobo* and *rp49* are nobo-qRT-PCR-F2 (5′-CGGTCCGCAGTTGCCTTATGC-3′), nobo-qRT-PCR-R2 (5′-GGACTAGGGTGGGAACACTGTGCTG-3′), rp49-qRT-PCR-F (5′-CGGATCGATATGCTAAGCTGT-3′) and rp49-qRT-PCR-R (5′-GCGCTTGTTCGATCCGTA-3′). Primers amplifying *rp49* were previously described (Foley et al., 1993).

In situ RNA hybridization

To generate a template for synthesising sense and antisense *nobo* RNA probes, the *nobo* ORF region was isolated from the pUAST-*nobo-HA* vector (described below) and inserted into pBluescriptII digested with *EcoR*I and *Not*I, whose sites are positioned in the multicloning site of the pUAST-HA vector. Plasmids for synthesising the *IMP-E1* and *IMP-L1* probes have been previously described (Niwa et al., 2004). Synthesis of DIG-labelled RNA probes and *in situ* hybridization were performed as previously described (Niwa et al., 2004).

Generation of anti-Nobo antibody and immunohistochemistry

Antibodies against the Nobo protein were raised in a guinea pig. A synthetic peptide (NH_2-MSQPKPILYYDERSPPVRSC-COOH) corresponding to residues 1-20 of the Nobo amino acid sequence (GenBank accession number AAF58397) was used for immunisation. Immunostaining for embryos, the brain-ring gland complex in third instar larvae, and the ovary in female adults was performed as previously described (Niwa et al., 2004; Shimada et al., 2011). The antibodies used were anti-Nobo antiserum (1:200 dilution), anti-FasIII 7G10 (obtained from the Developmental Studies Hybridoma Bank, Univ. of Iowa; 1:20 dilution), anti-guinea pig IgG antibody conjugated with Alexa488 (Life Technologies; 1:200 dilution), and

anti-mouse IgG antibody conjugated with Alexa488 (Life Technologies; 1:200 dilution).

UAS vectors, overexpression of genes and generation of transgenic strains

The GAL4/UAS system (Brand and Perrimon, 1993) was used to overexpress genes in *D. melanogaster*. To generate pUAST vectors to overexpress *nobo* and *nobo-Bm* (*B. mori GSTe7*), specific primers UAS-nobo-HA-F (5′-gtcagatctATGTCTCAGCCCAAGCCGATTTTG-3′), UAS-nobo-HA-R (5′-actgcggccgccCTCCACCTTCTCGGTGACTACCGCTG-3′), UAS-nobo-Bm-HA-F (5′-gtcagatctATGTCCATTGTTCGGTGTAATATG-3′), and UAS-nobo-Bm-HA-R (5′-actgcggccgccGTTTGGCTTGTAAAGACTCATAAAATA-3′) were used for PCR to add *Bgl*II and *Not*I sites to the 5′ and 3′ ends (shown underlined), respectively, of each of the cDNA fragments corresponding to CDSs. Template cDNAs were reverse transcribed using total RNAs of the ring gland from *D. melanogaster* and the PG from *B. mori* (KINSHU x SHOWA F_1 hybrid) using Prime Script Reverse Transcriptase (TaKaRa). Total RNA from the PG of *B. mori* was provided by Dr. T. Shinoda (The National Institute of Agrobiological Sciences). PCR was performed using Prime Star HS DNA polymerase (TaKaRa). The amplified CDS regions of

nobo and *nobo-Bm* were digested with *Bgl*II and *Not*I, and then ligated into a pUAST-HA vector carrying a sequence coding three tandem HA tags at the C terminal (Niwa et al., 2004). To generate overexpression vectors of *GSTe4* and *GSTe12*, each CDS region was ligated into the pWALIUM10-moe vector (purchased from Harvard RNAi Center; http://www.flyrnai.org/TRiP-HOME.html). Specific primers UAS-GstE4-CDS-F (5′-agtcagatctATGGGTAAGATATCGCTATAC-3′), UAS-GstE4-CDS-R (5′-tcagtctagaTTACGAAACTATGGTGAAG-3′), UAS-GstE12-CDS-F (5′-agtcagatctATGTCAAAGCCAGCTCTGTATT-3′), and UAS-GstE12-CDS-R (5′-tcagtctagaCTACTTGCCACGGTTTTCTG-3′) were used for PCR to add *Bgl*II and *Xba*I sites to the 5′ and 3′ ends (shown underlined), respectively, of each of the cDNA fragments corresponding to CDSs. Transformants were generated using the phiC31 integrase system in the *P{CaryP}attP40* strain. To establish w^+ transformants of pUAST and pWALIUM10-moe, injection was requested to Best Gene.

Generation of the gene-targeted $nobo^{KO}$ allele

Gene-targeting of *nobo* was carried out by the ends-out method (Rong and Golic, 2000) using the pP{EndsOut2} and pBSII-70w (Matsuo et al., 2007) vectors provided

by the Drosophila Genomics Resource Center and Dr. T. Matsuo (Tokyo Metropolitan Univ.), respectively. 5′ upstream and 3′ downstream regions of *nobo* were amplified by PCR with specific primer pairs noboKO5F-*Xho*I (5′-CTCGAGTAGCCTGATGCTGTCTCCAAGC-3′), noboKO5R-loxP-*Not*I (5′-GCGGCCGCATAACTTCGTATAGCATACATTATACGAAGTTATTAGCCACAGT ACTGATTGATGGTGG-3′), noboKO3F-loxP-*Hind*III (5′-AAGCTTATAACTTCGTATAATGTATGCTATACGAAGTTATCACCGAGAAGGT GGAGTAGCACTAG-3′), and noboKO3R-SphI (5′-GCATGCCCAAACGTAAAATCCTGAGACGTAAGC-3′).

5′ upstream and 3′ downstream PCR fragments were subcloned into pP{EndsOut2} with a *hsp70-white* mini-gene fragment excited from the pBSII-70w with *Not*I and *Hind*III. The *nobo* targeting vector was injected into the *w*⁻ strain using standard protocols. Targeting crosses were carried out as described by the Sekelsky Lab (http://sekelsky.bio.unc.edu/Research/Targeting/Targeting.html). The *nobo* knock-out strain was back-crossed to the w^{1118} strain for five generations.

Embryonic cuticle preparation

Embryonic cuticle preparation was carried out as previously described

(Nüsslein-Volhard et al., 1984). Homozygous *nobo*^{KO} (*nobo*^{KO}/*nobo*^{KO}) embryos were obtained as offspring from *nobo*^{KO}/*CyO Act5C-GFP* parents. Eggs were laid on a grape juice plate with yeast paste. From 21 to 27 hours after egg-laying, embryos were digested with bleach to dechorionation and then fixed with glycerol-acetic acid (1:4) on a glass dish at 60°C for 1 hour. Fixed embryos were transferred onto side glass and mounted with Hoyer's medium and then incubated at 60°C overnight.

20E rescue of *nobo*^{KO} embryos

The 20E rescue experiment was performed as previously described (Niwa et al., 2010; Ono et al., 2006). 20E was purchased from Sigma. Homozygous *nobo*^{KO} (*nobo*^{KO}/*nobo*^{KO}) embryos were obtained as offspring from *nobo*^{KO}/*CyO Act5C-GFP* parents. From 6 to 9 hours after egg-laying, embryos were collected and digested with bleach for dechorionation. Dechorionated embryos were incubated with or without 100 μM 20E in PBS containing 2% Tween-20 at room temperature for 3 hours. After 24 hours, hatched homozygous *nobo*^{KO}/*nobo*^{KO} laevae were distinguished from heterozygous *nobo*^{KO} (*nobo*^{KO}/*CyO Act5C-GFP*) laevae by assessing the presence or absence of a GFP signal under a fluorescence dissection microscope (Leica MZFLIII).

Rescue experiments with ecdysteroid intermediates

Cholesterol and 7-dehydrocholesterol (7dC) were purchased from Wako and Sigma, respectively. For maternal sterol rescue experiments, I used a *nobo*^{KO} strain balanced with the *CyO Act5C-GFP* balancer chromosome, which carries a GFP expression construct. Female flies were kept on a standard cornmeal food with yeast pastes containing 0.5%(w/w) sterol in 3.3%(w/w) ethanol (50 mg of yeast paste, 0.75 mg of sterol, 95 μl of water and 5 μl of ethanol) for 3 days. Then, female flies were crossed with male flies of the same strain, which were reared on standard cornmeal food without steroidal supplement, and were left to lay eggs on grape agar plates for 1 day. At 24 hours after egg laying (AEL), the genotype of each hatched larva was scored by assessing the presence or absence of a GFP signal under a fluorescence dissection microscope MZFLIII (Leica). The *nobo*^{KO} allele was also distinguished from its wild-type sequence by genomic PCR with a specific primer pair noboKO-genotype-F (5′-GGCGCGAGAGGTACATTGTTTAGC-3′) and noboKO-genotype-R (5′-CACTTGGCAGCTGGAAAGTCAGAG-3′), also shown in (Fig. 2a). Feeding rescue experiments for rescued *nobo*^{KO} and *nobo* RNAi larvae were conducted as previously described (Niwa et al., 2010; Yoshiyama et al., 2006).

Transgenic RNAi experiment and scoring of developmental progression

UAS-nobo-IR and w^{1118} flies were crossed with *UAS-dicer2; UAS-phm-GAL4#22* flies. Eggs were laid on grape plates with yeast pastes at 25°C for 4 hours. 50 hatched first instar larvae were transferred into a single vial with standard cornmeal food. Every 24 hours, developmental stages were scored by tracheal morphology as previously described (Niwa et al., 2010).

Transgenic RNAi experiment using several GAL4 lines

UAS-dicer2; UAS-nobo-IR (#40316); and *UAS-nobo-IR; UAS-dicer2 (#101884)* lines were crossed with *2-286-GAL4* (Timmons et al., 1997), *Act5c-GAL4* (Namiki et al., 2005), *Akh-GAL4* (Lee and Park, 2004), *Aug21-GAL4* (Siegmund and Korge, 2001), *daughterless-GAL4* (Wodarz et al., 1995), *elav-GAL4* (Luo et al., 1994), *NPC1b-GAL4* (Voght et al., 2007), *phm-GAL4 (w1)* (Ono et al., 2006), and *tub-GAL4* (Lee and Luo, 1999). Gnenotypes of progeny flies were distinguished by dominant markers on balancer chromosomes.

Fluorescence analysis of cholesterol distribution by 22-NBD-cholesterol

To assess the incorporation of cholesterol and to visualise its distribution, we

conducted *in vitro* incubation of the brain-ring gland complexes dissected from third instar larvae with 22-(*N*-(7-Nitrobenz-2-oxa-1,3-diazol-4-yl)amino)-23,24-bisnor-5-cholen-3β-ol (22-NBD-cholesterol; Life Technologies). 22-NBD-cholesterol was dissolved in 100% ethanol at 2 mM concentration for a stock solution. To avoid the lethality of *nobo* RNAi at the earlier larval stages, we utilised the *GAL80^{ts}* technique (McGuire et al., 2003) to conditionally suppress GAL4 transcriptional activity during first and second instar larval development. In this experiment, control (*w^{1118}; UAS-dicer2/+; phm-GAL4#22 tubP-GAL80^{ts}/+*) and conditional *nobo* RNAi flies (*w^{1118}; UAS-dicer2/UAS-nobo-IR; phm-GAL4#22 tubP-GAL80^{ts}/+*) were used. The first instar larvae were transferred into standard cornmeal food and reared at 21°C for 2 days. After 2 days, larvae were then reared at 25°C for an additional 3 days, allowing the larvae to reach the third instar stage. The third instar larvae were dissected in PBS, and the brain-ring gland complexes were transferred into Schneider's Drosophila Medium (Life Technologies) containing 10% fatal bovine serum, 100 U/ml penicillin (Wako), and 100 μg/ml Streptomycin (Wako). After an incubation at 25°C for 10 min, the medium was replaced with a fresh medium containing 0.5% 22-NBD-cholesterol stock solution, which achieved a 10 μM

22-NBD-cholesterol with 0.5% final ethanol concentration. Then, tissues were incubated at 25°C for 6 hours in a dark condition. Tissues were washed with PBS twice and mounted. A 488 nm laser was used for excitation of 22-NBD-cholesterol fluorescence, and fluorescence emission was selected by a 490-555 nm-band pass filter. Fluorescence images were obtained with an LSM 700 laser-scanning confocal microscope (Zeiss).

A mass-spectrometric quantification of 20E and sterols

For the measurement of 20E in whole bodies of control (*w^{1118}; UAS-dicer2/+; UAS-phm-GAL4#22/+*) and *nobo* RNAi flies (*w^{1118}; UAS-dicer2/ UAS-nobo-IR; UAS-phm-GAL4#22/+*), the second instar larvae (56–64 hours AEL) of each genotype were collected. Then the wet weight of each sample was measured, and the samples were frozen with liquid nitrogen and stored at -80°C until measurement. For the measurement of sterol levels in the RG, the RG samples from the control and *nobo* RNAi larvae were collected as described above in "Fluorescence analysis of cholesterol distribution by 22-NBD-cholesterol". Ten ring glands were collected from third instar larvae and then transferred into a single glass vial on dry ice. All samples were stored at -80°C until measurement. For each genotype, 10

independent samples, each containing 10 ring glands, were used for analysis. Extraction of steroids, HPLC fractionation, and mass-spectrometric analyses were performed as previously described (Hikiba et al., 2013; Igarashi et al., 2011), except for a minor modification of the sterol quantification and the mobile phase conditions (run time: 0-12 min, acetonitrile isocratic, flow rate: 300 μl/min). In the mass-spectrometric analyses, the exact quantification range was 0.1221-31.25 ng/mL. In these experimental conditions, the limit of quantification of 20E was 0.916 pg of 20E/mg of wet weight sample. Mass-spectrometric analyses for 20E and sterol quantification were conducted by Dr. M. Iga (University of Tokyo) and Dr. F. Igarashi (University of Tokyo), respectively.

GST phylogenetic analysis

The rootless tree was generated based on the entire amino acid sequence of *Drosophila melanogaster* Nobo and the other 277 GST proteins by the neighbour-joining method through the MEGA5 program (Tamura et al., 2011). The names and GenBank accession numbers of GST proteins in this tree are listed in a Supplementary table. GST amino acid sequences were collected from 13 species including Aa, *Aedes aegypti*; Ag, *Anopheles gambiae*; Tc, *Tribolium castaneum*; Cq,

Culex quinquefasciatus; Dm, *Drosophila melanogaster*; Bm, *Bombyx mori*; Ph, *Pediculus humanus corporis*; Nv, *Nasonia vitripennis*; Am, *Apis mellifera*; Ap, *Acyrthosiphon pisum*; Dp, *Danaus plexippus*; Ce, *Caenorhabditis elegans*; and Hs, *Homo sapiens.*

Refereneces

Awata, N., Morisaki, M. and Ikekawa, N. (1975). Carbon-carbon bond cleavage of fucosterol-24, 28-oxide by cell-free extracts of silkworm Bombyx mori. *Biochem. Biophys. Res. Commun.* **64**, 157–161.

Ayres, C. F. J., Ayres, C., Müller, P., Dyer, N., Wilding, C. S., Wilding, C., Rigden, D. J., Rigden, D., Donnelly, M. J. and Donnelly, M. (2011). Comparative genomics of the anopheline glutathione S-transferase epsilon cluster. *PLoS One* **6**, e29237.

Board, P. G. and Menon, D. (2013). Glutathione transferases, regulators of cellular metabolism and physiology. *Biochim. Biophys. Acta* **1830**, 3267–88.

Brand, A. H. and Perrimon, N. (1993). Targeted gene expression as a means of altering cell fates and generating dominant phenotypes. *Development* **118**, 401–415.

Bujold, M., Gopalakrishnan, A., Nally, E. and King-Jones, K. (2010). Nuclear receptor DHR96 acts as a sentinel for low cholesterol concentrations in Drosophila melanogaster. *Mol. Cell. Biol.* **30**, 793–805.

Caldwell, P. E., Walkiewicz, M. and Stern, M. (2005). Ras activity in the Drosophila prothoracic gland regulates body size and developmental rate via ecdysone release. *Curr. Biol.* **15**, 1785–95.

Carvalho, M., Schwudke, D., Sampaio, J. L., Palm, W., Riezman, I., Dey, G., Gupta, G. D., Mayor, S., Riezman, H., Shevchenko, A., et al. (2010). Survival strategies of a sterol auxotroph. *Development* **137**, 3675–85.

Chanut-Delalande, H., Hashimoto, Y., Pelissier-Monier, A., Spokony, R., Dib, A., Kondo, T., Bohère, J., Niimi, K., Latapie, Y., Inagaki, S., et al. (2014). Pri peptides are mediators of ecdysone for the temporal control of development. *Nat. Cell Biol.* **16**, 1035–1044.

Chávez, V. M., Marqués, G., Delbecque, J. P., Kobayashi, K., Hollingsworth, M., Burr, J., Natzle, J. E. and O'Connor, M. B. (2000). The Drosophila disembodied gene controls late embryonic morphogenesis and codes for a cytochrome P450 enzyme that regulates embryonic ecdysone levels. *Development* **127**, 4115–4126.

Chen, H., Ma, Z., Liu, Z., Tian, Y., Xiang, Y., Wang, C., Scott, M. P. and Huang, X. (2009). Case studies of ends-out gene targeting in Drosophila. *Genesis* **47**, 305–8.

Chowen, J. A., Garcia-Segura, L. M., Gonzalez-Parra, S. and Argente, J. (1996). Sex steroid effects on the development and functioning of the growth hormone axis. *Cell. Mol. Neurobiol.* **16**, 297–310.

Ciufo, L. F., Murray, P. a, Thompson, A., Rigden, D. J. and Rees, H. H. (2011). Characterisation of a desmosterol reductase involved in phytosterol dealkylation in the silkworm, Bombyx mori. *PLoS One* **6**, e21316.

Clark, A. J. and Bloch, K. (1959). The Absence of Sterol Synthesis in Insects. *J. Biol. Chem.* **234**, 2578–2582.

Clark, A. G., Eisen, M. B., Smith, D. R., Bergman, C. M., Oliver, B., Markow, T. a, Kaufman, T. C., Kellis, M., Gelbart, W., Iyer, V. N., et al. (2007). Evolution of genes and genomes on the Drosophila phylogeny. *Nature* **450**, 203–18.

Claudius, A. K., Romani, P., Lamkemeyer, T., Jindra, M. and Uhlirova, M. (2014). Unexpected Role of the Steroid-Deficiency Protein Ecdysoneless in Pre-mRNA Splicing. *PLoS Genet.* **10**, e1004287.

Dobrosotskaya, I. Y., Seegmiller, A. C., Brown, M. S., Goldstein, J. L. and Rawson, R. B. (2002). Regulation of SREBP processing and membrane lipid production by phospholipids in Drosophila. *Science* **296**, 879–883.

Enayati, a a, Ranson, H. and Hemingway, J. (2005). Insect glutathione transferases and insecticide resistance. *Insect Mol. Biol.* **14**, 3–8.

Enya, S., Ameku, T., Igarashi, F., Iga, M., Kataoka, H., Shinoda, T. and Niwa, R. (2014). A Halloween gene noppera-bo encodes a glutathione S-transferase essential for ecdysteroid biosynthesis via regulating the behaviour of cholesterol in Drosophila. *Sci. Rep.* **4**, 6586.

Fedulova, N., Raffalli-Mathieu, F. and Mannervik, B. (2010). Porcine glutathione transferase Alpha 2-2 is a human GST A3-3 analogue that catalyses steroid double-bond isomerization. *Biochem. J.* **431**, 159–67.

Fluegel, M. L., Parker, T. J. and Pallanck, L. J. (2006). Mutations of a Drosophila NPC1 gene confer sterol and ecdysone metabolic defects. *Genetics* **172**, 185–196.

Foley, K. P., Leonard, M. W. and Engel, J. D. (1993). Quantitation of RNA using the polymerase chain reaction. *Trends Genet.* **9**, 380–5.

Freeman, M. R., Dobritsa, A., Gaines, P., Segraves, W. A. and Carlson, J. R. (1999). The dare gene: steroid hormone production, olfactory behavior, and neural degeneration in Drosophila. *Development* **126**, 4591–4602.

Friedman, R. (2011). Genomic organization of the glutathione S-transferase family in insects. *Mol. Phylogenet. Evol.* **61**, 924–932.

Frova, C. (2006). Glutathione transferases in the genomics era: new insights and perspectives. *Biomol. Eng.* **23**, 149–169.

Fujimoto, Y., Morisaki, M. and Ikekawa, N. (1980). Stereochemical importance of fucosterol epoxide in the conversion of sitosterol into cholesterol in the silkworm Bombyx mori. *Biochemistry* **19**, 1065–1069.

Gaziova, I., Bonnette, P. C., Henrich, V. C. and Jindra, M. (2004). Cell-autonomous roles of the ecdysoneless gene in Drosophila development and oogenesis. *Development* **131**, 2715–2725.

Gibbens, Y. Y., Warren, J. T., Gilbert, L. I. and O'Connor, M. B. (2011). Neuroendocrine regulation of Drosophila metamorphosis requires TGFbeta/Activin signaling. *Development* **138**, 2693–2703.

Gilbert, L. I. (2004). Halloween genes encode P450 enzymes that mediate steroid hormone biosynthesis in Drosophila melanogaster. *Mol. Cell. Endocrinol.* **215**, 1–10.

Gilbert, L. I., Rybczynski, R. and Warren, J. T. (2002). Control and biochemical nature of the ecdysteroidogenic pathway. *Annu. Rev. Entomol.* **47**, 883–916.

Grieneisen, M. L., Warren, J. T. and Gilbert, L. I. (1993). Early steps in ecdysteroid biosynthesis: evidence for the involvement of cytochrome P-450 enzymes. *Insect Biochem. Mol. Biol.* **23**, 13–23.

Hayes, J. D. and Pulford, D. J. (1995). The glutathione S-transferase supergene family: regulation of GST and the contribution of the isoenzymes to cancer chemoprotection and drug resistance. *Crit. Rev. Biochem. Mol. Biol.* **30**, 445–600.

Hikiba, J., Ogihara, M. H., Iga, M., Saito, K., Fujimoto, Y., Suzuki, M. and Kataoka, H. (2013). Simultaneous quantification of individual intermediate steroids in silkworm ecdysone biosynthesis by liquid chromatography-tandem mass spectrometry with multiple reaction monitoring. *J. Chromatogr. B Anal. Technol. Biomed. Life Sci.* **915-916**, 52–56.

Horner, M. a, Pardee, K., Liu, S., King-Jones, K., Lajoie, G., Edwards, A., Krause, H. M. and Thummel, C. S. (2009). The Drosophila DHR96 nuclear receptor binds cholesterol and regulates cholesterol homeostasis. *Genes Dev.* **23**, 2711–2716.

Hu, M.-C., Hsu, N.-C., El Hadj, N. Ben, Pai, C.-I., Chu, H.-P., Wang, C.-K. L. and Chung, B.-C. (2002). Steroid deficiency syndromes in mice with targeted disruption of Cyp11a1. *Mol. Endocrinol.* **16**, 1943–1950.

Huang, X., Suyama, K., Buchanan, J., Zhu, A. J. and Scott, M. P. (2005). A Drosophila model of the Niemann-Pick type C lysosome storage disease: dnpc1a is required for molting and sterol homeostasis. *Development* **132**, 5115–5124.

Huang, X., Warren, J. T., Buchanan, J., Gilbert, L. I. and Scott, M. P. (2007). Drosophila Niemann-Pick type C-2 genes control sterol homeostasis and steroid biosynthesis: a model of human neurodegenerative disease. *Development* **134**, 3733–3742.

Igarashi, F., Hikiba, J., Ogihara, M. H., Nakaoka, T., Suzuki, M. and Kataoka, H. (2011). A highly specific and sensitive quantification analysis of the sterols in silkworm larvae by high performance liquid chromatography-atmospheric pressure chemical ionization-tandem mass spectrometry. *Anal. Biochem.* **419**, 123–132.

Jarcho, M., Parvy, J., Warren, J. T., Petryk, A., Marque, G., Dauphin-villemant, C., Connor, M. B. O. and Gilbert, L. I. (2002). Molecular and biochemical characterization of two P450 enzymes in the ecdysteroidogenic pathway of Drosophila melanogaster. *Proc. Natl. Acad. Sci. U. S. A.* **99**, 11043–11048.

Johansson, A. S. and Mannervik, B. (2001). Human glutathione transferase A3-3, a highly efficient catalyst of double-bond isomerization in the biosynthetic pathway of steroid hormones. *J. Biol. Chem.* **276**, 33061–33065.

Jürgens, G., Wieschaus, E., Nüsslein-Volhard, C. and Kluding, H. (1984). Mutations affecting the pattern of the larval cuticle in Drosophila melanogaster II. Zygotic loci on the third chromosome. *Roux's Arch. Dev. Biol.* **193**, 283–295.

Karlson, P. (1996). On the hormonal control of insect metamorphosis. A historical review. *Int. J. Dev. Biol.* **40**, 93–96.

Kennerdell, J. R. and Carthew, R. W. (2000). Heritable gene silencing in Drosophila using double-stranded RNA. *Nat. Biotechnol.* **18**, 896–898.

Kim, J., Suh, H., Kim, S., Kim, K., Ahn, C. and Yim, J. (2006). Identification and characteristics of the structural gene for the Drosophila eye colour mutant sepia, encoding PDA synthase, a member of the omega class glutathione S-transferases. *Biochem. J.* **398**, 451–460.

Kim, K., Kim, S.-H., Kim, J., Kim, H. and Yim, J. (2012). Glutathione s-transferase omega 1 activity is sufficient to suppress neurodegeneration in a Drosophila model of Parkinson disease. *J. Biol. Chem.* **287**, 6628–41.

King-Jones, K. and Thummel, C. S. (2005). Nuclear receptors--a perspective from Drosophila. *Nat. Rev. Genet.* **6**, 311–323.

Kurzchalia, T. V and Ward, S. (2003). Why do worms need cholesterol? *Nat. Cell Biol.* **5**, 684–688.

Laborde, E. (2010). Glutathione transferases as mediators of signaling pathways involved in cell proliferation and cell death. *Cell Death Differ.* **17**, 1373–80.

Lee, T. and Luo, L. (1999). Mosaic Analysis with a Repressible Neurotechnique Cell Marker for Studies of Gene Function in Neuronal Morphogenesis. **22**, 451–461.

Lee, G. and Park, J. H. (2004). Hemolymph sugar homeostasis and starvation-induced hyperactivity affected by genetic manipulations of the adipokinetic hormone-encoding gene in Drosophila melanogaster. *Genetics* **167**, 311–323.

Luo, L., Liao, Y. J., Jan, L. Y. and Jan, Y. N. (1994). Distinct morphogenetic functions of similar small GTPases: Drosophila Drac1 is involved in axonal outgrowth and myoblast fusion. *Genes Dev.* **8**, 1787–1802.

Mangelsdorf, D. J., Thummel, C., Beato, M., Herrlich, P., Schutz, G., Umesono, K., Blumberg, B., Kastner, P., Mark, M., Chambon, P., et al. (1995). The nuclear receptor superfamily: the second decade. *Cell* **83**, 835–839.

Markstein, M., Pitsouli, C., Villalta, C., Celniker, S. E. and Perrimon, N. (2008). Exploiting position effects and the gypsy retrovirus insulator to engineer precisely expressed transgenes. *Nat. Genet.* **40**, 476–83.

Maróy, P., Kaufmann, G. and Dübendorfer, A. (1988). Embryonic ecdysteroids of Drosophila melanogaster. *J. Insect Physiol.* **34**, 633–637.

Matsuo, T., Sugaya, S., Yasukawa, J., Aigaki, T. and Fuyama, Y. (2007). Odorant-binding proteins OBP57d and OBP57e affect taste perception and host-plant preference in Drosophila sechellia. *PLoS Biol.* **5**, 0985–0996.

McBrayer, Z., Ono, H., Shimell, M., Parvy, J.-P., Beckstead, R. B., Warren, J. T., Thummel, C. S., Dauphin-Villemant, C., Gilbert, L. I. and O'Connor, M. B. (2007). Prothoracicotropic hormone regulates developmental timing and body size in Drosophila. *Dev. Cell* **13**, 857–71.

McGuire, S. E., Le, P. T., Osborn, A. J., Matsumoto, K. and Davis, R. L. (2003). Spatiotemporal rescue of memory dysfunction in Drosophila. *Science* **302**, 1765–1768.

Namiki, T., Niwa, R., Sakudoh, T., Shirai, K.-I., Takeuchi, H. and Kataoka, H. (2005). Cytochrome P450 CYP307A1/Spook: a regulator for ecdysone synthesis in insects. *Biochem. Biophys. Res. Commun.* **337**, 367–74.

Nebert, D. W., Wikvall, K., Miller, W. L. and B, P. T. R. S. (2013). Human cytochromes P450 in health and disease Human cytochromes P450 in health and disease. *Philos. Trans. R. Soc. Lond. B. Biol. Sci.*

Niwa, R. and Niwa, Y. S. (2011). The Fruit Fly Drosophila melanogaster as a Model System to Study Cholesterol Metabolism and Homeostasis. *Cholesterol* **2011**, 176802.

Niwa, R. and Niwa, Y. S. (2014). Enzymes for ecdysteroid biosynthesis: their biological functions in insects and beyond. *Biosci. Biotechnol. Biochem.* **78**, 1283–1292.

Niwa, R., Matsuda, T., Yoshiyama, T., Namiki, T., Mita, K., Fujimoto, Y. and Kataoka, H. (2004). CYP306A1, a cytochrome P450 enzyme, is essential for ecdysteroid biosynthesis in the prothoracic glands of Bombyx and Drosophila. *J. Biol. Chem.* **279**, 35942–35949.

Niwa, R., Sakudoh, T., Namiki, T., Saida, K., Fujimoto, Y. and Kataoka, H. (2005). The ecdysteroidogenic P450 Cyp302a1/disembodied from the silkworm, Bombyx mori, is transcriptionally regulated by prothoracicotropic hormone. *Insect Mol. Biol.* **14**, 563–571.

Niwa, R., Namiki, T., Ito, K., Shimada-Niwa, Y., Kiuchi, M., Kawaoka, S., Kayukawa, T., Banno, Y., Fujimoto, Y., Shigenobu, S., et al. (2010). Non-molting glossy/shroud encodes a short-chain dehydrogenase/reductase that functions in the "Black Box" of the ecdysteroid biosynthesis pathway. *Development* **137**, 1991–1999.

Nüsslein-Volhard, C., Wieschaus, E. and Kluding, H. (1984). Mutations affecting the pattern of the larval cuticle in Drosophila melanogaster I. Zygotic loci on the second chromosome. *Roux's Arch. Dev. Biol.* **193**, 267–282.

Ohkama-Ohtsu, N., Sasaki-Sekimoto, Y., Oikawa, A., Jikumaru, Y., Shinoda, S., Inoue, E., Kamide, Y., Yokoyama, T., Hirai, M. Y., Shirasu, K., et al. (2011). 12-oxo-phytodienoic acid-glutathione conjugate is transported into the vacuole in Arabidopsis. *Plant Cell Physiol.* **52**, 205–9.

Ono, H., Rewitz, K. F., Shinoda, T., Itoyama, K., Petryk, A., Rybczynski, R., Jarcho, M., Warren, J. T., Marques, G., Shimell, M. J., et al. (2006). Spook and Spookier code for stage-specific components of the ecdysone biosynthetic pathway in Diptera. *Dev. Biol.* **298**, 555–570.

Ou, Q., Magico, A. and King-Jones, K. (2011). Nuclear receptor DHR4 controls the timing of steroid hormone pulses during Drosophila development. *PLoS Biol.* **9**, e1001160.

Petryk, A., Warren, J. T., Marques, G., Jarcho, M. P., Gilbert, L. I., Kahler, J., Parvy, J. P., Li, Y., Dauphin-Villemant, C. and O'Connor, M. B. (2003). Shade is the Drosophila P450 enzyme that mediates the hydroxylation of ecdysone to the steroid insect molting hormone 20-hydroxyecdysone. *Proc. Natl. Acad. Sci. U. S. A.* **100**, 13773–13778.

Raffalli-Mathieu, F., Orre, C., Stridsberg, M., Hansson Edalat, M. and Mannervik, B. (2008). Targeting human glutathione transferase A3-3 attenuates progesterone production in human steroidogenic cells. *Biochem. J.* **414**, 103–9.

Rewitz, K. F., Styrishave, B., Løbner-Olesen, A. and Andersen, O. (2006). Marine invertebrate cytochrome P450: Emerging insights from vertebrate and insect analogies. *Comp. Biochem. Physiol. - C Toxicol. Pharmacol.* **143**, 363–381.

Rewitz, K. F., O'Connor, M. B. and Gilbert, L. I. (2007). Molecular evolution of the insect Halloween family of cytochrome P450s: Phylogeny, gene organization and functional conservation. *Insect Biochem. Mol. Biol.* **37**, 741–753.

Rewitz, K. F., Yamanaka, N., Gilbert, L. I. and O'Connor, M. B. (2009). The insect neuropeptide PTTH activates receptor tyrosine kinase torso to initiate metamorphosis. *Science* **326**, 1403–5.

Riddiford, L. M. (1993). Hormones and Drosophila development. *Dev. Drosoph. melanogaster* 899–939.

Rodenburg, K. W. and Van der Horst, D. J. (2005). Lipoprotein-mediated lipid transport in insects: analogy to the mammalian lipid carrier system and novel concepts for the functioning of LDL receptor family members. *Biochim. Biophys. Acta* **1736**, 10–29.

Rong, Y. S. and Golic, K. G. (2000). Gene Targeting by Homologous Recombination in Drosophila. *Science (80-.).* **288**, 2013–2018.

Rosenbaum, A. I. and Maxfield, F. R. (2011). Niemann-Pick type C disease: Molecular mechanisms and potential therapeutic approaches. *J. Neurochem.* **116**, 789–795.

Roth, G. E., Gierl, M. S., Vollborn, L., Meise, M., Lintermann, R. and Korge, G. (2004). The Drosophila gene Start1: a putative cholesterol transporter and key regulator of ecdysteroid synthesis. *Proc. Natl. Acad. Sci. U. S. A.* **101**, 1601–1606.

Saisawang, C., Wongsantichon, J. and Ketterman, A. J. (2012). A preliminary characterization of the cytosolic glutathione transferase proteome from Drosophila melanogaster. *Biochem. J.* **442**, 181–90.

Scheidt, H. a, Muller, P., Herrmann, A. and Huster, D. (2003). The potential of fluorescent and spin-labeled steroid analogs to mimic natural cholesterol. *J. Biol. Chem.* **278**, 45563–9.

Seegmiller, A., Dobrosotskaya, I. and Goldstein, J. (2002). The SREBP Pathway in Drosophila: Regulation by Palmitate, Not Sterols. *Dev. Cell* **2**, 229–238.

Shabab, M., Khan, S. a, Vogel, H., Heckel, D. G. and Boland, W. (2014). OPDA isomerase GST16 is involved in phytohormone detoxification and insect development. *FEBS J.* **281**, 2769–83.

Shimada, Y., Burn, K. M., Niwa, R. and Cooley, L. (2011). Reversible response of protein localization and microtubule organization to nutrient stress during Drosophila early oogenesis. *Dev. Biol.* **355**, 250–262.

Sieber, M. H. and Thummel, C. S. (2009). The DHR96 nuclear receptor controls triacylglycerol homeostasis in Drosophila. *Cell Metab.* **10**, 481–90.

Siegmund, T. and Korge, G. (2001). Innervation of the ring gland of Drosophila melanogaster. *J. Comp. Neurol.* **431**, 481–491.

Stocco, D. M. (2001). StAR protein and the regulation of steroid hormone biosynthesis. *Annu. Rev. Physiol.* **63**, 193–213.

Sun, Y., Li, H. and Huang, J.-R. (2012). Arabidopsis TT19 functions as a carrier to transport anthocyanin from the cytosol to tonoplasts. *Mol. Plant* **5**, 387–400.

Sun, X. Q., Zhang, M. X., Yu, J. Y., Jin, Y., Ling, B., Du, J. P., Li, G. H., Qin, Q. M. and Cai, Q. N. (2013). Glutathione S-Transferase of Brown Planthoppers (Nilaparvata lugens) Is Essential for Their Adaptation to Gramine-Containing Host Plants. *PLoS One* **8**, e64026.

Tamura, K., Peterson, D., Peterson, N., Stecher, G., Nei, M. and Kumar, S. (2011). MEGA5: Molecular Evolutionary Genetics Analysis Using Maximum Likelihood, Evolutionary Distance, and Maximum Parsimony Method. *Mol. Biol. Evol.* **28**, 2731–2739.

Tars, K., Olin, B. and Mannervik, B. (2010). Structural basis for featuring of steroid isomerase activity in alpha class glutathione transferases. *J. Mol. Biol.* **397**, 332–40.

Tew, K. D. and Townsend, D. M. (2012). Glutathione-S-Transferases As Determinants of Cell Survival and Death. *Antioxid. Redox Signal.* **17**, 1728–1737.

Tew, K. D., Manevich, Y., Grek, C., Xiong, Y., Uys, J. and Townsend, D. M. (2011). The role of glutathione S-transferase P in signaling pathways and S-glutathionylation in cancer. *Free Radic. Biol. Med.* **51**, 299–313.

Thummel, C. S. (2001). Molecular mechanisms of developmental timing in C. elegans and Drosophila. *Dev. Cell* **1**, 453–465.

Timmons, L., Becker, J., Barthmaier, P., Fyrberg, C., Shearn, A. and Fyrberg, E. (1997). Green fluorescent protein/beta-galactosidase double reporters for visualizing Drosophila gene expression patterns. *Dev. Genet.* **20**, 338–347.

Voght, S. P., Fluegel, M. L., Andrews, L. A. and Pallanck, L. J. (2007). Drosophila NPC1b promotes an early step in sterol absorption from the midgut epithelium. *Cell Metab.* **5**, 195–205.

Wang, X., Sato, R., Brown, M. S., Hua, X. and Goldstein, J. L. (1994). SREBP-1, a membrane-bound transcription factor released by sterol-regulated proteolysis. *Cell* **77**, 53–62.

Warren, J. T., Wismar, J., Subrahmanyam, B. and Gilbert, L. I. (2001). Woc (without children) gene control of ecdysone biosynthesis in Drosophila melanogaster. *Mol. Cell. Endocrinol.* **181**, 1–14.

Warren, J. T., Petryk, A., Marqués, G., Parvy, J.-P., Shinoda, T., Itoyama, K., Kobayashi, J., Jarcho, M., Li, Y., O'Connor, M. B., et al. (2004). Phantom encodes the 25-hydroxylase of Drosophila melanogaster and Bombyx mori: a P450 enzyme critical in ecdysone biosynthesis. *Insect Biochem. Mol. Biol.* **34**, 991–1010.

Warren, J. T., O'Connor, M. B. and Gilbert, L. I. (2009). Studies on the Black Box: incorporation of 3-oxo-7-dehydrocholesterol into ecdysteroids by Drosophila melanogaster and Manduca sexta. *Insect Biochem. Mol. Biol.* **39**, 677–687.

Wieschaus, E., Nüsslein-Volhard, C. and Jürgens, G. (1984). Mutations affecting the pattern of the larval cuticle in Drosophila melanogaster III. Zygotic loci on the X-chromosome and fourth chromosome. *Roux's Arch. Dev. Biol.* **193**, 296–307.

Wismar, J., Habtemichael, N., Warren, J. T., Dai, J. D., Gilbert, L. I. and Gateff, E. (2000). The mutation without children(rgl) causes ecdysteroid deficiency in third-instar larvae of Drosophila melanogaster. *Dev. Biol.* **226**, 1–17.

Wodarz, A., Hinz, U., Engelbert, M. and Knust, E. (1995). Expression of crumbs confers apical character on plasma membrane domains of ectodermal epithelia of Drosophila. *Cell* **82**, 67–76.

Yamanaka, N., Honda, N., Osato, N., Niwa, R., Mizoguchi, A. and Kataoka, H. (2007). Differential regulation of ecdysteroidogenic P450 gene expression in the silkworm, Bombyx mori. *Biosci. Biotechnol. Biochem.* **71**, 2808–2814.

Yamanaka, N., Rewitz, K. F. and O'Connor, M. B. (2013). Ecdysone control of developmental transitions: lessons from Drosophila research. *Annu. Rev. Entomol.* **58**, 497–516.

Yoshiyama, T., Namiki, T., Mita, K., Kataoka, H. and Niwa, R. (2006). Neverland is an evolutionally conserved Rieske-domain protein that is essential for ecdysone synthesis and insect growth. *Development* **133**, 2565–2574.

Yoshiyama-Yanagawa, T., Enya, S., Shimada-Niwa, Y., Yaguchi, S., Haramoto, Y., Matsuya, T., Shiomi, K., Sasakura, Y., Takahashi, S., Asashima, M., et al. (2011). The conserved Rieske oxygenase DAF-36/Neverland is a novel cholesterol-metabolizing enzyme. *J. Biol. Chem.* **286**, 25756–25762.

Yu, Q., Lu, C., Li, B., Fang, S., Zuo, W., Dai, F., Zhang, Z. and Xiang, Z. (2008). Identification, genomic organization and expression pattern of glutathione S-transferase in the silkworm, Bombyx mori. *Insect Biochem. Mol. Biol.* **38**, 1158–1164.

Tables

Table 1. Viability of *nobo^{KO}* animals with the expression of *nobo* and other GST genes.

The number of viable *nobo^{KO}/nobo^{KO}* adults was scored. Transgenes were driven by *phm-GAL4#22* driver. Each cross of parental males with parental females is indicated. Genetic markers of the *CyO* and *TM6B* balancer chromosomes are *Cy*$^{-}$ and *Hu*$^{-}$, respectively. *nobo^{KO}/nobo^{KO}* and viable control *nobo^{KO}/+* adults were *Cy*$^{+}$ *Hu*$^{+}$ and *Cy*$^{-}$ *Hu*$^{+}$, respectively.

Back ground	Transgene	Parents (males)	Parents (females)	Cy+, Hu+	Cy-, Hu+
nobo^{KO}	*nobo#1*	*w; nobo^{KO}/CyO; phm-GAL4#22/TM6B*	*w; nobo^{KO}/CyO; P{UAS-nobo-HA}#1/TM6B*	101	220
	nobo#2	*w; nobo^{KO}/CyO; phm-GAL4#22/TM6B*	*w; nobo^{KO}/CyO; P{UAS-nobo-HA}#2/TM6B*	124	255
	nobo#3	*w; nobo^{KO}/CyO; P{UAS-nobo-HA}#3/TM6B*	*w; nobo^{KO}/CyO; phm-GAL4#22/TM6B*	46	102
	nobo-Bm#1	*w; nobo^{KO}/CyO; phm-GAL4#22/TM6B*	*w; P{UAS-nobo-Bm-HA}#1 nobo^{KO}/CyO*	85	377
	nobo-Bm#5	*w; nobo^{KO}/CyO; P{UAS-nobo-Bm-HA}#5/TM6B*	*w; nobo^{KO}/CyO; phm-GAL4#22/TM6B*	77	348
	CG6673B	*w; nobo^{KO}/CyO; P{UAS-CG6673B}/TM6B*	*w; nobo^{KO}/CyO; phm-GAL4#22/TM6B*	0	105
	GSTe4	*w; nobo^{KO}/CyO; phm-GAL4#22/TM6B*	*w; P{UAS-GSTe4}attP40 nobo^{KO}/CyO*	0	102
	GSTe12	*w; nobo^{KO}/CyO; phm-GAL4#22/TM6B*	*w; P{UAS-GSTe12}attP40 nobo^{KO}/CyO*	0	117

Table 2. Rescue of homozygous *nobo*^{KO} embryos by incubation with 20E.

The numbers of the first instar larvae and percentage of rescued mutant are indicated. Embryos of the indicated genotype were incubated with or without 100 μM 20E. Genotypes were assessed by the presence of GFP signal.

	Number of the 1st instar larvae		% of rescued
Steroid	*nobo*^{KO}/*nobo*^{KO}	*nobo*^{KO}/*CyO Act-GFP*	mutant
None	0	96	0
20E	64	145	44.1

Table 3. Lethality induced *UAS-nobo-IR* driven by several GAL4 lines

The number of viable adults was scored. *UAS-nobo-IR* lines were driven by listed GAL4 drivers. Values in parentheses indicate the number of viable non-RNAi control progeny from the parental strains in the same experimental batches. Progenies from crosses with daughterless-GAL4 and NPC1b-GAL4 lines were all lethal and viable respectively.

		UAS-nobo-IR line	
GAL4 line	Expression tissue	#101884	#40316
2-286	PG, salivaly gland and a part of neurons	0 [172]	0 [284]
Act5c	Ubiquitous	0 [144]	0 [86]
Akh	CC	128 [107]	133 [112]
Aug21	CA	216 [135]	56 [11]
daughterless	Ubiquitous	0	0
elav	Neurons	111 [130]	140 [148]
NPC1b	Midgut	viable	viable
phm (w1)	PG	0 [151]	0 [115]
tub	Ubiquitous	0 [154]	0 [115]

Table 4. Rescue of homozygous *nobo*^{KO} embryos by maternal sterol administration.
The numbers of the first instar larvae that were offspring of *nobo*^{KO}*/CyO Act-GFP* mothers, which were fed standard cornmeal food with yeast pastes containing 0.5%(w/w) each sterol, and % of rescued mutant are indicated. Genotype was assessed by the presence of a GFP signal and genomic PCR results (See Supplementary fig. S2).

	Number of first instar larvae		% of rescued
Sterol	*nobo*^{KO}/*nobo*^{KO}	*nobo*^{KO}/ *CyO Act-GFP*	mutant
None	0	44	0
C	79	129	61.2
7dC	63	118	53.4

Table 5. Rescue of homozygous *nobo*^{KO} larvae by oral sterol administration

The numbers of the first, second and third instar larvae of the *nobo*^{KO} homozygous larvae, which were fed standard cornmeal food with yeast pastes containing 0.5%(w/w) sterol/steroid supplement, are indicated. Homozygous *nobo*^{KO} larvae were obtained by maternal administration of cholesterol to homozygous *nobo*^{KO} embryos as shown in Table 3. Larval instars were scored at 72 hours AEL.

	Larval instar		
Sterol/steroid	First	Second	Third
None	16	2	0
C	18	4	1
7dC	18	6	0
20E	1	4	19

Table 6. Viability of *nobo* RNAi animals with the expression of *nobo-Bm* and other GST genes.

The number of viable *nobo* RNAi adults was scored. Transgenes were driven by *phm-GAL4#22* driver. Each cross of parental males with parental females is indicated. Genetic markers of the *CyO*, *TM6B* and *TM3* balancer chromosomes are Cy^-, Hu^- and Sb^-, respectively. *nobo* RNAi and viable non-RNAi adults were Cy^+ Hu^+ Sb^+ and Hu^-, respectively.

Back ground	Transgene	Parents (males)	Parents (females)	CyO+, Hu+, Sb+	Hu-
nobo RNAi	*nobo-Bm#1*	*w; UAS-dicer2; phm-GAL4#22/TM6*	*w; P{UAS-nobo-Bm-HA}#1/CyO; P{UAS-nobo-IR}#40316/TM6B*	120	498
	nobo-Bm#2	*w; UAS-dicer2; phm-GAL4#22/TM6*	*w; P{UAS-nobo-Bm-HA}#2/CyO; P{UAS-nobo-IR}#40316/TM6B*	105	350
	GSTe4	*w; UAS-dicer2; phm-GAL4#22/TM6*	*w; P{UAS-GSTe4}attP40/CyO; P{UAS-nobo-IR}#40316/TM6B*	0	92
	GSTe12	*w; UAS-dicer2; phm-GAL4#22/TM6*	*w; P{UAS-GSTe12}attP40/CyO; P{UAS-nobo-IR}#40316/TM6B*	0	105
	sepia	*w; UAS-dicer2; phm-GAL4#22/TM6*	*w; P{UAS-sepia}; P{UAS-nobo-IR}#40316/TM6B*	0	249
	CG6673A	*w; UAS-dicer2; phm-GAL4#22/TM6*	*w; P{UAS-CG6673A}; P{UAS-nobo-IR}#40316/TM6B*	0	120
	CG6673B	*w; UAS-dicer2; phm-GAL4#22/TM6*	*w; P{UAS-nobo-IR}#101884; P{UAS-CG6673B}/TM6B*	0	278
	CG6662	*w; UAS-dicer2; phm-GAL4#22/TM6*	*w; P{UAS-CG6662}; P{UAS-nobo-IR}#40316/TM3 Sb*	0	107

Figures and figure legends

Figure I. Ecdysteroid and insect development

(a) Structure of ecdysone.

(b) Ecdysteroid pulses regulate developmental transitions such as embryogenesis, molting, and metamorphosis in *D. melanogaster*. Developmental stages and the ecdysteroid titer corresponding to each stage are shown. Adapted from Riddiford, 1993.

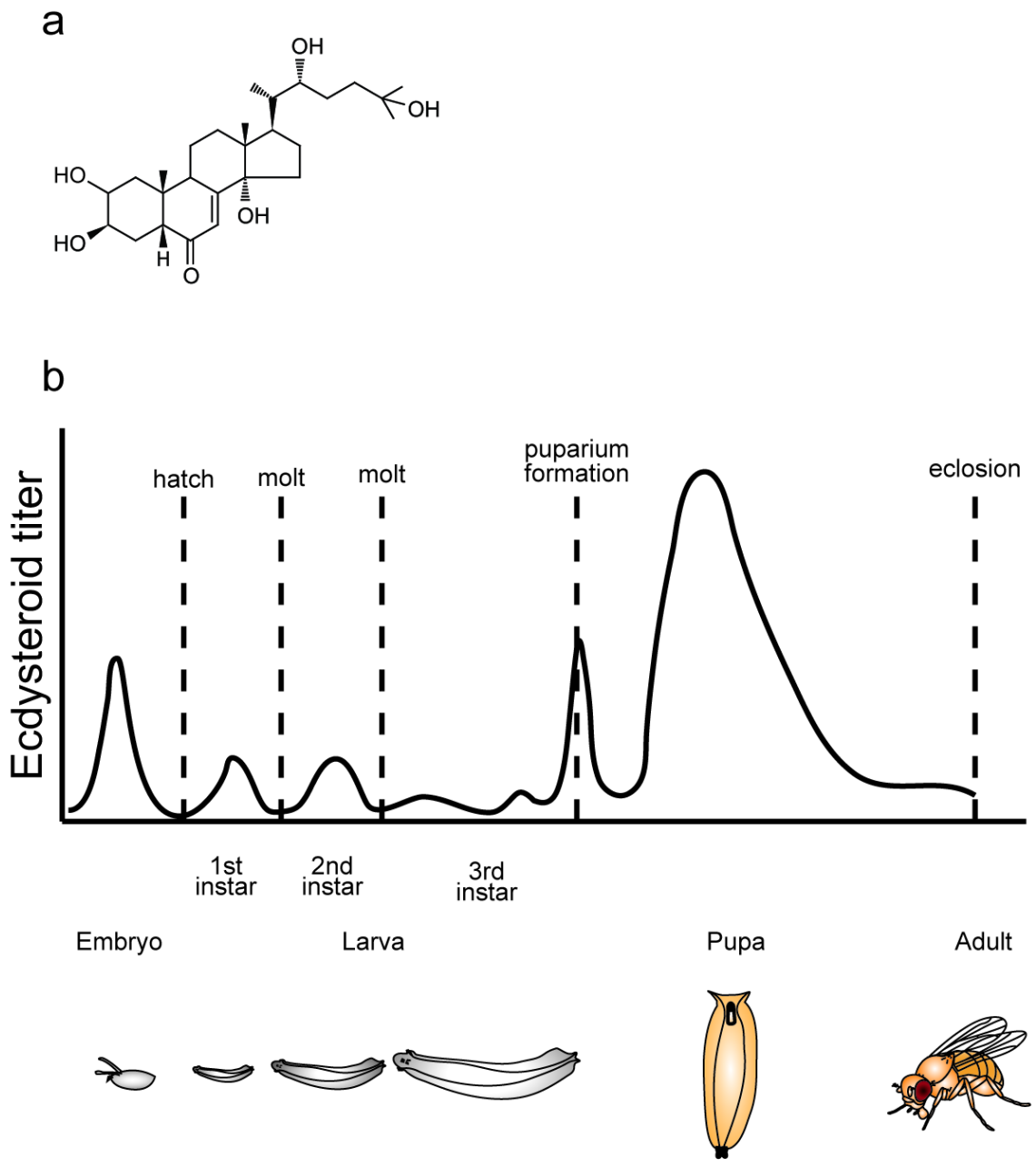

Figure I. Ecdysteroid and insect development

Figure II. Ecdysone biosynthesis pathway

20E and its intermediates and ecdysone biosynthesis enzymes are shown. Adapted from Ryusuke Niwa & Niwa, 2014.

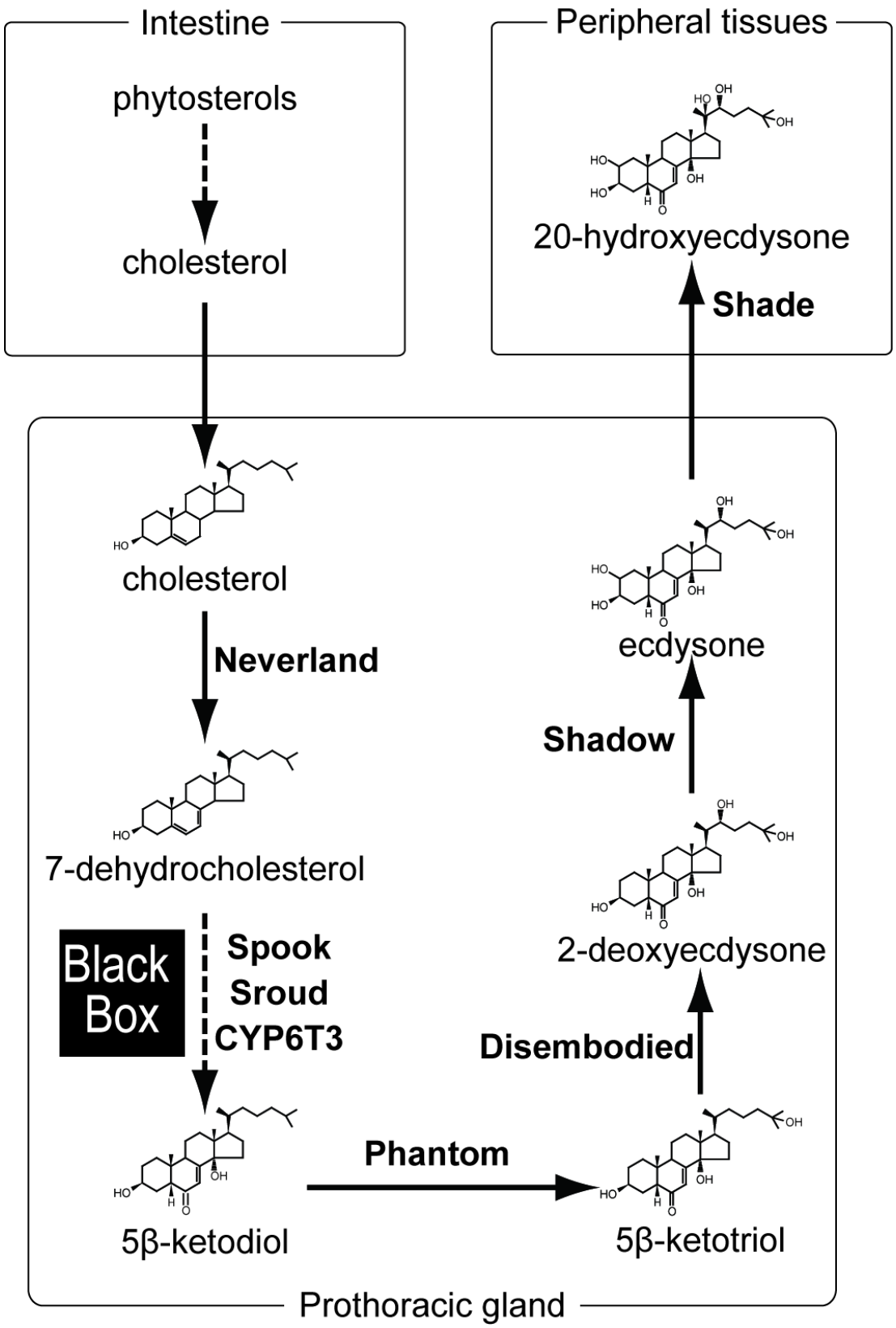

Figure II. Ecdysone biosynthesis pathway

Figure 1. Expression pattern of *CG4688/nobo* in larval and adult tissues.

(a) The expression levels of *CG4688/nobo* in several tissues from wandering third instar larvae and adult flies were quantified by qRT-PCR. BR, brain; RG, ring gland; FB, fat body; SG, salivary gland; ID, imaginal discs; IN, intestine; TS, testis; OV, ovary. Each error bar represents the s.e.m. from three independent samples. The normalized *nobo* mRNA level in the RG is set as 1.

(b-e) Localization of *nobo* mRNA and Nobo protein in the PG and the adult ovaries. (b, b') *In situ* hybridization with the *nobo* antisense RNA probe and (c, c') anti-Nobo immunoreactivity were detected in the PG cells but not in other regions in the brain-ring gland complex of wandering third instar larvae. The inset of (c) shows a bright-field image of the same specimen. (b') and (c') show higher magnifications of the ring gland in (b) and (c), respectively. The arrow and arrowheads indicate the corpus allatum (CA) and the corpus cardiacum (CC), respectively. (d) The presence of *nobo* mRNA and (e) Nobo protein were strongly detected in the follicle cells of stage 8 (St.8) ovarioles in developing egg chambers. (d, e) *In situ* hybridization and immunohistochemical analyses in the adult ovary were carried out by Mr. Tomotsune Ameku. Scale bars: (b, c) 100 μm, (d, e) 25 μm.

(f) qRT-PCR analysis of the *nobo* transcripts in the PGs isolated from 140±6 hour AEL third instar larvae of control, *torso* RNAi, and *ptth*-expression neuron-ablated (*ptth>grim*) animals. Each error bar represents the s.e.m. from three independent samples. The *nobo* expression levels in each control were set as 1. *, $P<0.05$ with Student's *t*-test.

a-f are reprinted from Enya et al., 2014.

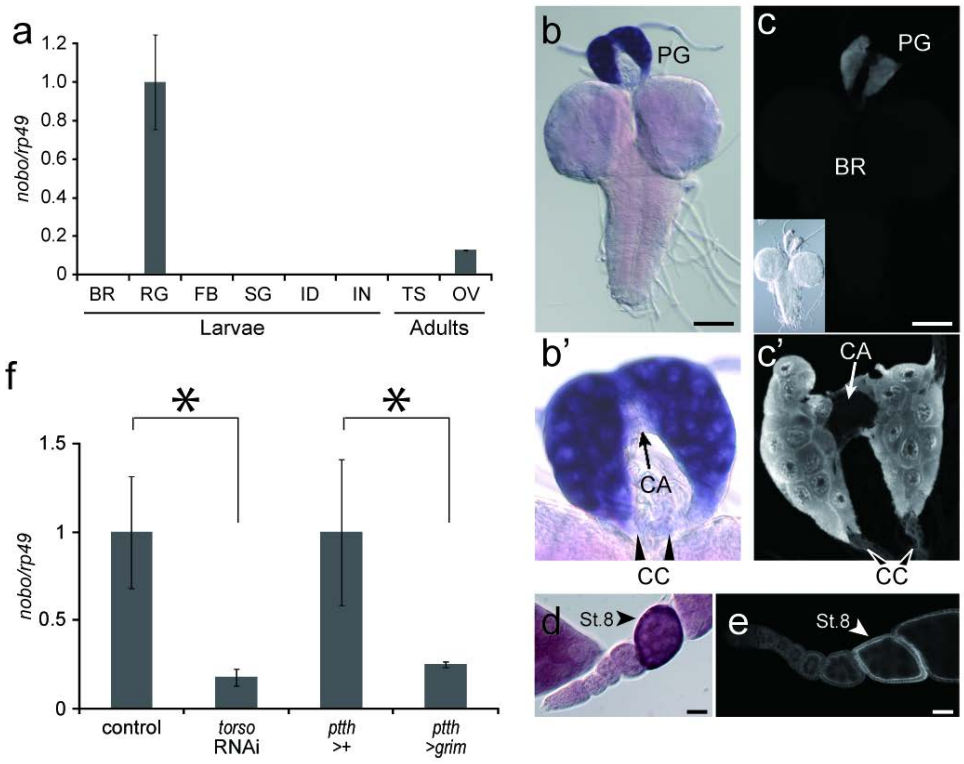

Figure 1. Expression pattern of *CG4688/nobo* in larval and adult tissues.

Figure 2. Expression pattern of *nobo* in embryonic stages.

(a) The temporal expression profile of *nobo* during embryogenesis. A black line and white bars are schematic representations of the embryonic ecdysteroid titre and *sro* expression levels, respectively, based on published data (Maróy et al., 1988; Niwa et al., 2010). The normalized *nobo* and *sro* mRNA levels at 2-4 hours AEL are set as 1. (b-g) *In situ* RNA hybridisation analysis in embryos with *nobo* antisense probe. Lateral (b-f) and ventral (g) views are shown. (b-f) *nobo* mRNA was observed in epidermal cells during stages 5-11. (f) At stage 11, *nobo* mRNA was detected in the amnioserosa (arrow), which is thought to synthesise ecdysteroids. (g) At stage 16 and later, a *nobo* signal was detected in the PG cells (arrowheads). An inset with a higher magnification of the PG. Scale bar: 100 μm.

a-g are reprinted from Enya et al., 2014.

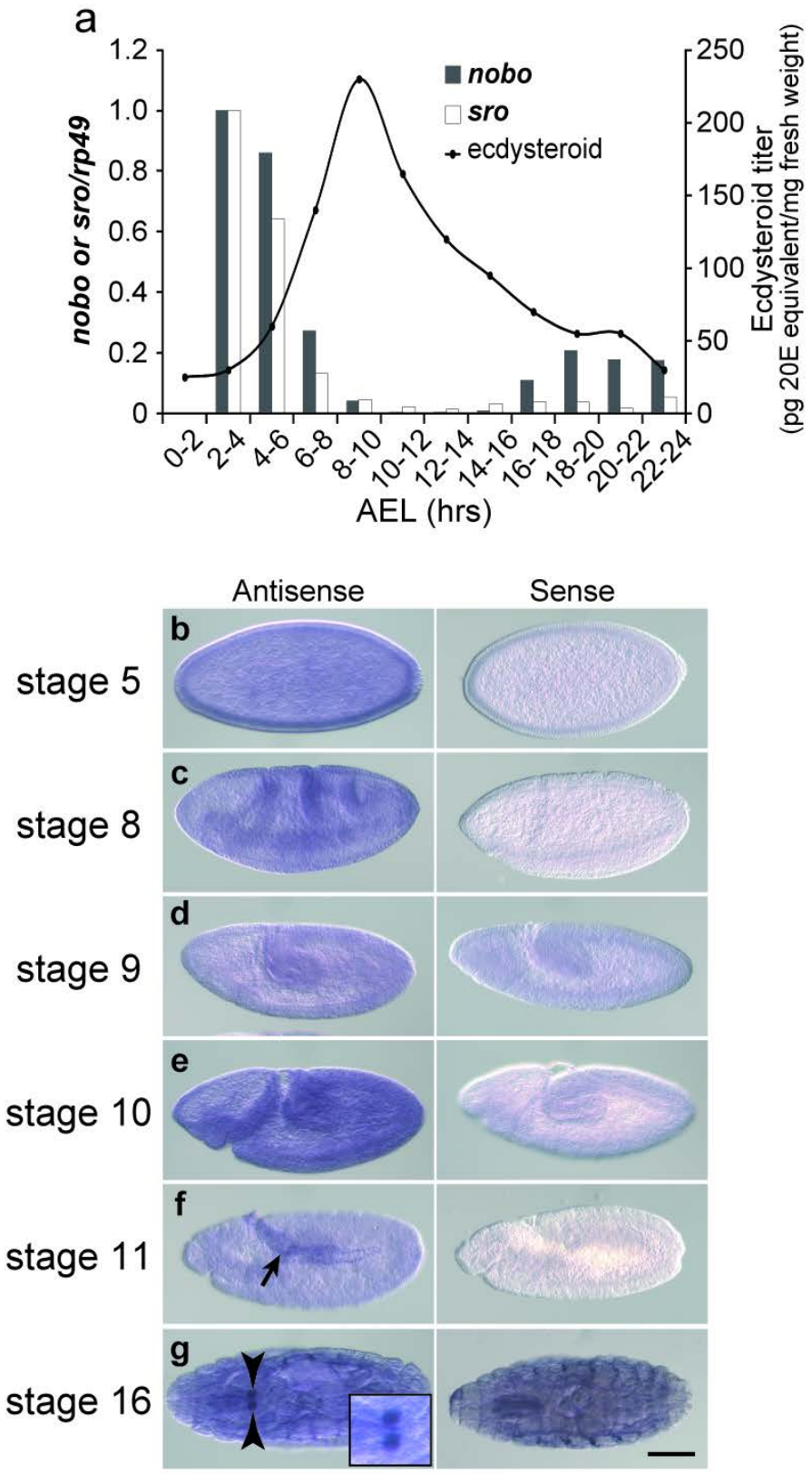

Figure 2. Expression pattern of *nobo* in embryonic stages.

Figure 3. Generation and morphology of *nobo*^{KO} homozygous mutant embryos.

(a) Genomic and exon-intron structures of the *nobo* (*CG4688)* loci of the wild-type and *nobo* knock-out (*nobo*^{KO}) strains. White and black boxes indicate the coding sequence and the untranslated regions, respectively. *CG4649* is a gene located next to *nobo*. Dashed arrows indicate orientations of the genes. In the *nobo*^{KO} allele, 1,033 bp of the *nobo* gene region was replaced with a gene-targeting construct including the *hsp70::mini-white* marker cassette with loxP sites, resulting in a 680 bp deletion in the entire (696 bp) *nobo* coding sequence. Arrows 'F' and 'R' indicate the positions of the genotyping primers used in Fig. 7.

(b, c) Dark-field images of embryonic cuticles from (b) *nobo*^{KO} heterozygous (*nobo*^{KO}*/+*) and (c) homozygous (*nobo*^{KO}*/nobo*^{KO}) embryos.

(d-g) Anti-FasIII antibody staining to visualise overall embryo morphology. (d, f) *nobo*^{KO}*/+* embryos. (e, g) *nobo*^{KO}*/nobo*^{KO} embryos. (e) The bracket indicates defective head involution. (g) The arrow and the arrowhead indicate the dorsal open phenotype and abnormal gut looping, respectively.

(a-g) are reprinted from Enya et al., 2014.

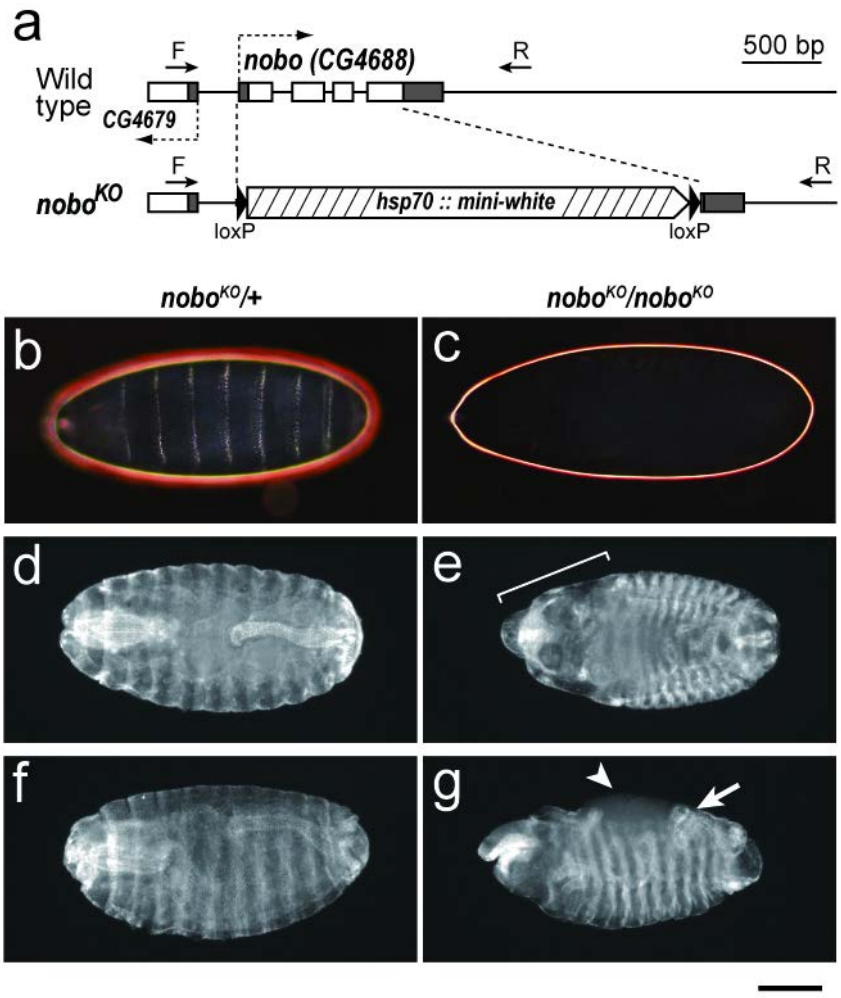

Figure 3. Generation and morphology of *nobo*^{KO} homozygous mutant embryos.

Figure 4. Expression of ecdysone-inducible genes in *nobo*^{KO} mutant embryos.

(a-d) Expression patterns of (a, b) *IMP-E1* and (c, d) *IMP-L1* in stage 14 embryos. (a, c) *nobo*^{KO}*/+* embryos. (b, d) *nobo*^{KO}*/nobo*^{KO} embryos. These data show that the *nobo* mutant exhibited severe reductions in these 20E-inducible genes.

Scale bars: 100 μm for all images.

a-d are reprinted from Enya et al., 2014.

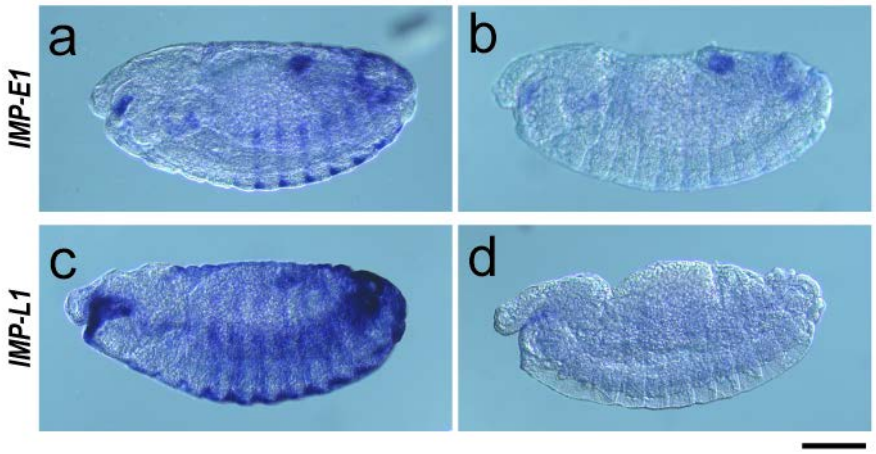

Figure 4. Expression of ecdysone-inducible genes in *nobo*^{KO} mutant embryos.

Figure 5. *nobo*^{KO} mutant flies expressing transgenic *nobo*.

Genotype of left and right flies are *w; nobo*^{KO}*/nobo*^{KO}*; phm-GAL4#22/UAS-nobo-HA#1* and *w; nobo*^{KO}*/CyO; phm-GAL4#22/UAS-nobo-HA#1,* respectively. The cross scheme is described in Table 1.

w; nobo^{KO}/ nobo^{KO}; phm>nobo-HA *w; nobo^{KO}/ CyO ; phm>nobo-HA*

Figure 5. *nobo^{KO}* mutant flies expressing transgenic *nobo*.

Figure 6. Larval lethality and developmental arrest phenotype of *nobo* RNAi larvae.

(a) Expression levels of control and *nobo* RNAi first instar larvae collected at 36 hours AEL. Each error bar represents the s.e.m. from three independent samples. The normalized *nobo* expression level in the control was set as 1. *, $P<0.05$ with Student's *t*-test.

(b,c) The survival rate and developmental progression of (b) control (N=150) and (c) *nobo* RNAi animals (N=100). L1, L2, and L3 indicate the first, second, and third instar larvae, respectively.

(d-f) Comparison of body size and developmental stage between control (right) and *nobo* RNAi (left) animals. Typically, control animals became the second instar larva, the third instar larva, and pupa at (d) 48 hours, (e) 72 hours, and (f) 144 hours AEL, respectively. In contrast, *nobo* RNAi animals in these photos are the first, second, and second instar larvae, which were collected at each of the same time points, respectively. Scale bar: 1 mm.

(a-f) are reprinted from Enya et al., 2014.

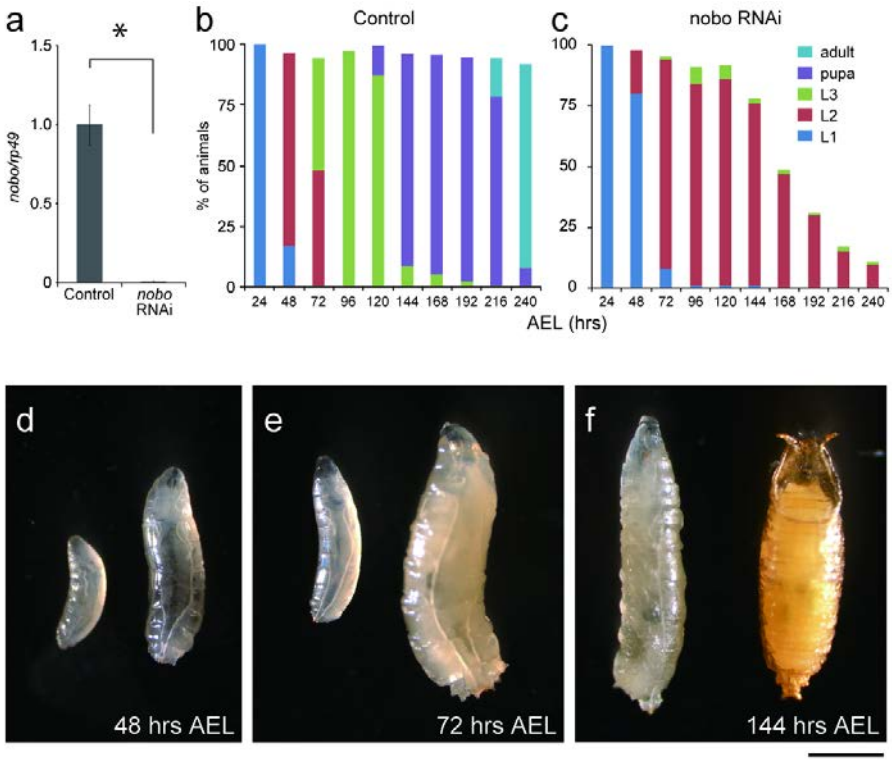

Figure 6. Larval lethality and developmental arrest phenotype of *nobo* RNAi larvae.

Figure 7. PCR genotyping analysis of first instar larvae of the wild-type Oregon R, *nobo*^{KO} heterozygous animals (balanced with *CyO*) and *nobo*^{KO} homozygous animals rescued by maternally supplied cholesterol and 7dC.

nobo^{KO} homozygous animals were collected as GFP-negative offspring of *nobo*^{KO}/*CyO-GFP* parents that were fed cholesterol (C) or 7dC. For each genotype, PCR products from three single first instar larvae were used for agarose gel electrophoresis. The PCR primers for genotyping are illustrated in Fig. 2a ('F' and 'R'). Black and magenta arrowheads indicate PCR bands corresponding to the wild-type (2260 bp) and *nobo*^{KO} (4047 bp) alleles, respectively. Lanes 1-3, Oregon R without any sterol supplements; lanes 4-6, *nobo*^{KO}/*CyO* without any sterol supplements; lanes 7-9, *nobo*^{KO}/*nobo*^{KO} first instar larvae that were maternally supplied with cholesterol; and lanes 10-12, *nobo*^{KO}/*nobo*^{KO} first instar larvae that were maternally supplied with 7dC.

This figure is reprinted from Enya et al., 2014.

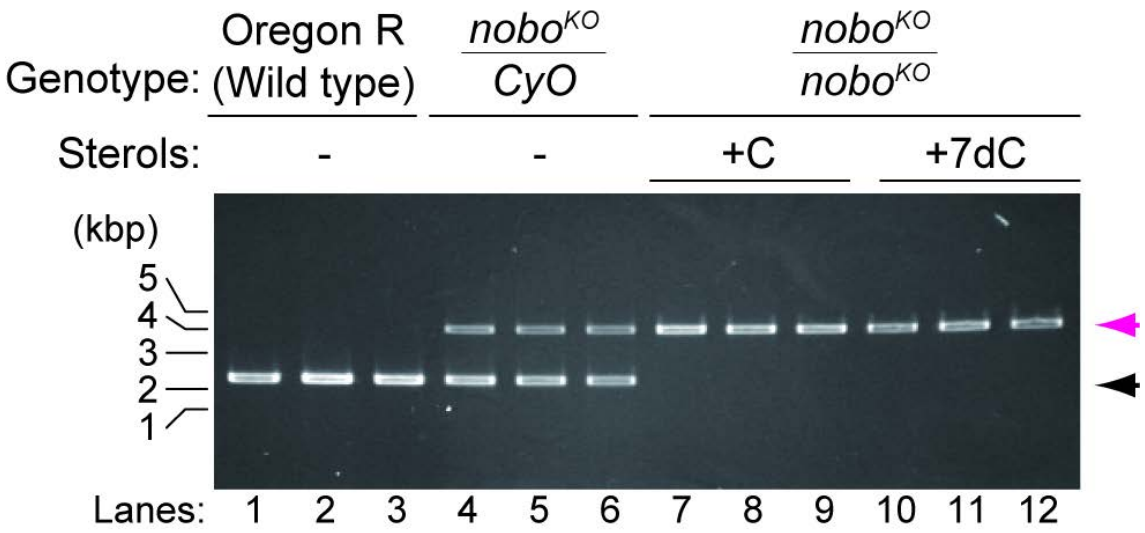

Figure 7. PCR genotyping analysis of first instar larvae of the wild-type Oregon R, *nobo*^{KO} heterozygous animals (balanced with *CyO*) and *nobo*^{KO} homozygous animals rescued by maternally supplied cholesterol and 7dC.

Figure 8. Feeding rescue experiments and abnormal cholesterol accumulation in *nobo* RNAi animals.

(a) Feeding rescue experiments for *nobo* RNAi larvae. *nobo* RNAi and control larvae were fed yeast paste supplemented with ethanol (EtOH, for negative control), cholesterol (C), 7-dehydrocholesterol (7dC) or 20E throughout their larval development. The concentration of each supplemented steroid in yeast paste was 0.5%(w/w) (See Methods section for more details). The percentage of living animals at 240 hours AEL in each experimental condition was scored. N>30 for each experiment. Inset photo shows *nobo* RNAi animals at 240 hours AEL, which were raised on food with EtOH- (right) and 20E-supplemented (left) food, respectively. The larva (right) was at the 2nd instar stage.

(b) Sterol amounts in the RG isolated from control and *nobo* RNAi larvae. C, cholesterol; βsito, β-sitosterol; Ergo, ergosterol; Campe, campesterol. 7dC amounts were under the detectable level in our experimental conditions, and thus, the 7dC data were not included in this graph. N=10 for each genotype. *, $P<0.05$ with Student's *t*-test. n.s., not significant. Note that the higher level of β-sitosterol was observed in *nobo* RNAi PG cells, but the difference was not statistically significant. The mass-spectrometric analysis was carried out by Dr. Fumihiko Igarashi.

(c, d) Fluorescence and bright-field (inset) images of the PG from (c) control and (d) *nobo* RNAi animals incubated with 22-NBD-cholesterol. White dotted lines indicate the PG area. Scale bar: 50 μm.

a-d are reprinted from Enya et al., 2014.

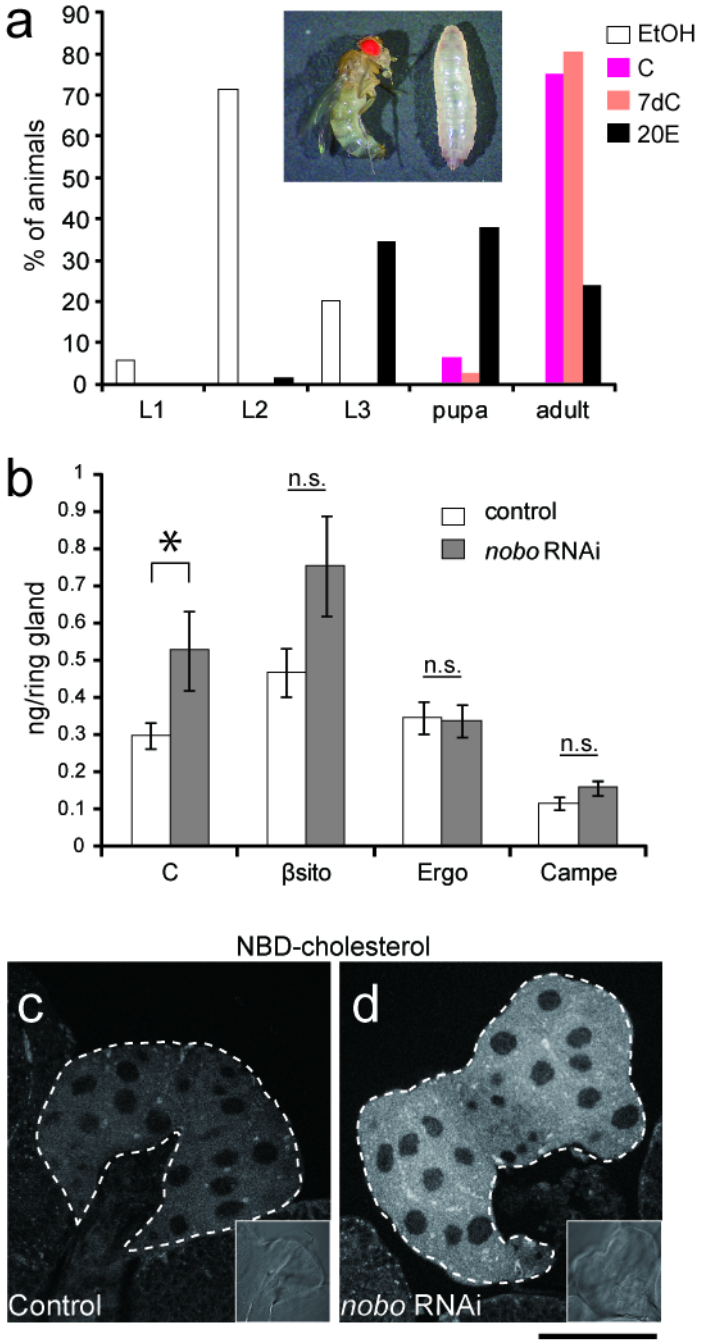

Figure 8. Feeding rescue experiments and abnormal cholesterol accumulation in *nobo* RNAi animals.

Figure 9. A phylogenetic tree shows the relationship between Nobo and other GST proteins.

(a) The rootless tree was generated based on the entire amino acid sequence of *Drosophila melanogaster* Nobo and the other 277 GST proteins by the neighbour-joining method through the MEGA5 program (Tamura et al., 2011). The names and GenBank accession numbers of GST proteins in this tree are listed in a Supplementary table. Aa, *Aedes aegypti*; Ag, *Anopheles gambiae*; Tc, *Tribolium castaneum*; Cq, *Culex quinquefasciatus*; Dm, *Drosophila melanogaster*; Bm, *Bombyx mori*; Ph, *Pediculus humanus corporis*; Nv, *Nasonia vitripennis*; Am, *Apis mellifera*; Ap, *Acyrthosiphon pisum*; Dp, *Danaus plexippus*; Ce, *Caenorhabditis elegans*; and Hs, *Homo sapiens*. Pink and blue areas indicate clades that include *nobo* subfamily genes and human GSTA3 family genes, respectively.

(b) A phylogenetic clade of *nobo* subfamily genes, which was derived from (a). Each number indicates the bootstrap value for each branch.

A scale bar shows the number of amino acid substitutions per site between the two sequences.

a-b are reprinted from Enya et al., 2014.

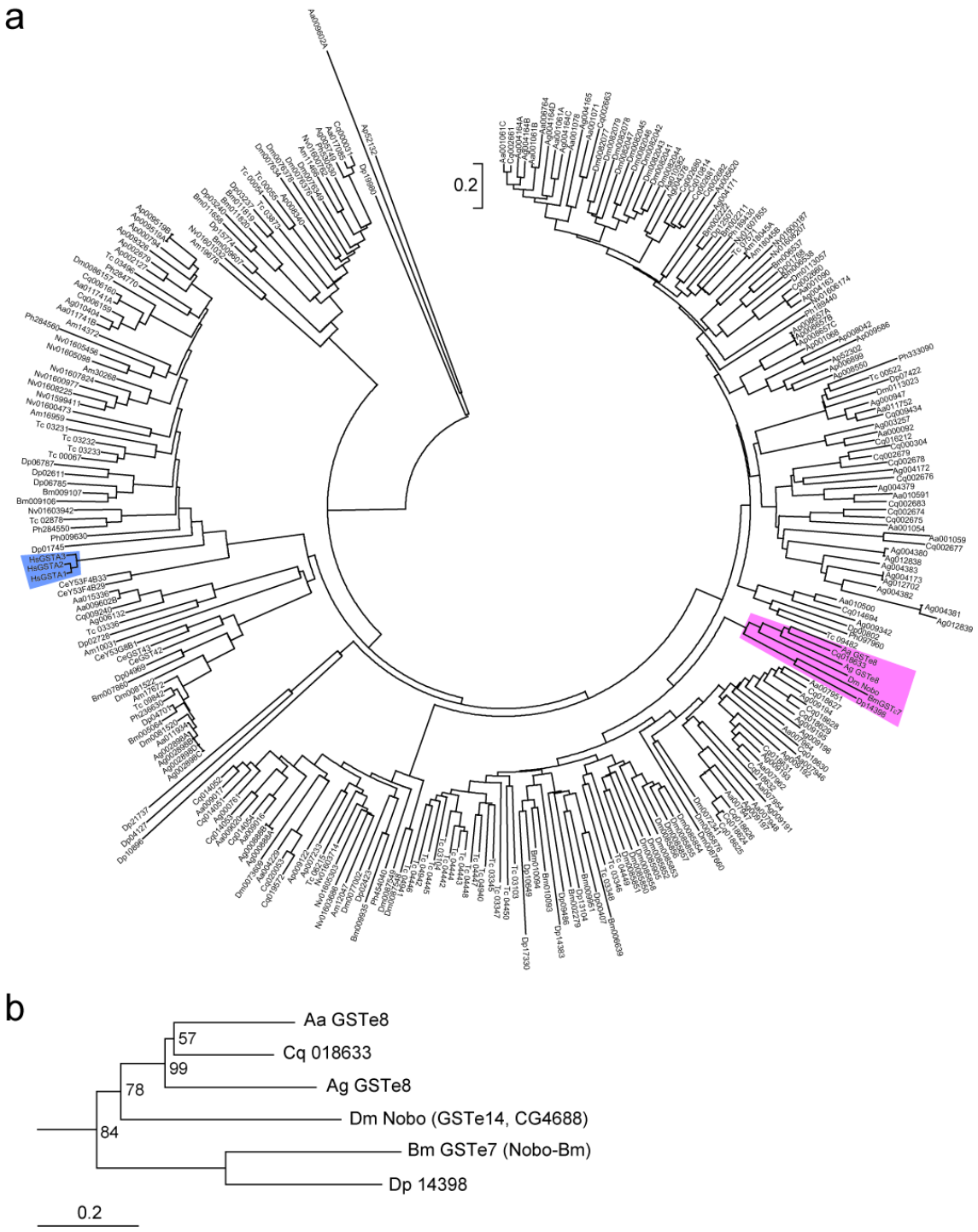

Figure 9. A phylogenetic tree shows the relationship between Nobo and other GST proteins.

Figure 10. Function model of Nobo in the PG cell

On the left side, Nobo positively regulates cholesterol trafficking in the wild type PG cells. Cholesterol is thought to be transported from cell membrane to mitochondria through golgi and ER. Then cholesterol is converted by a series of ecdysteroidogenic enzymes localized in ER and mitochondria.

On the right side, loss of *nobo* function causes defects in cholesterol transport and cholesterol accumulation. Then, necessary amounts of cholesterol for ecdysone biosynthesis are not transported to ER and mitochondria causing ecdysone deficiency.

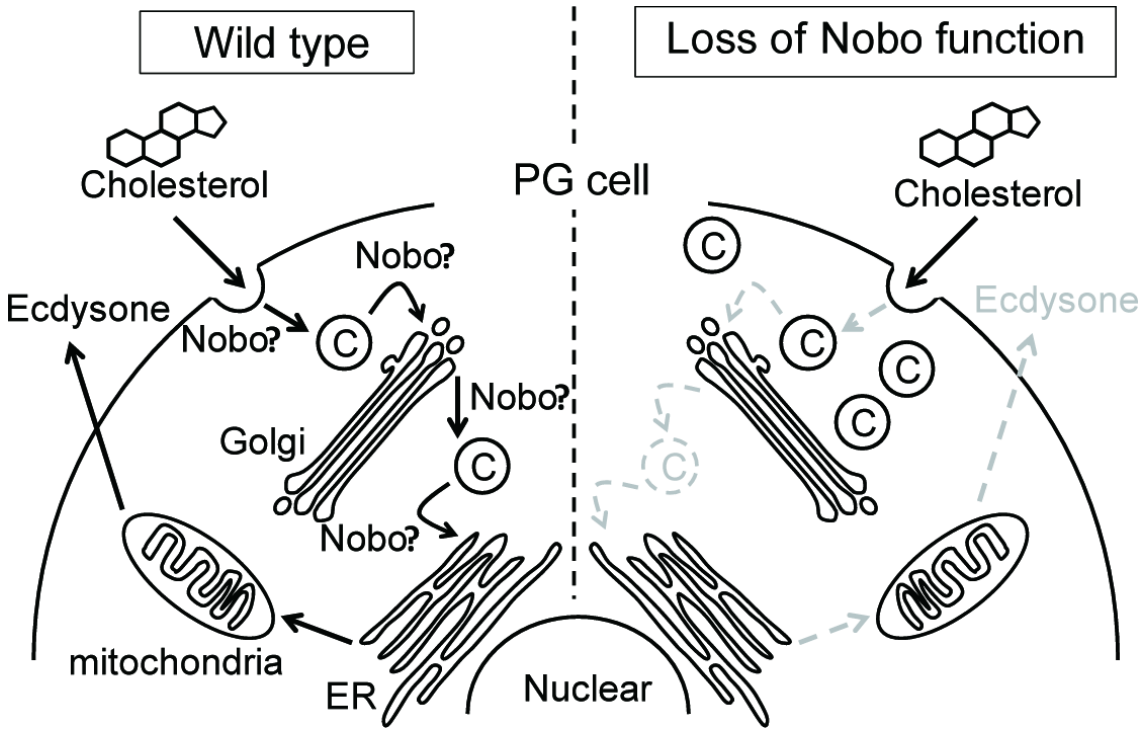

Figure 10. Function model of Nobo in the PG cell

Acknowledgement

I thank Dr. Ryusuke Niwa for guiding me for six years as my supervisor.

I thank Niwa laboratory members: Dr. Ryusuke Niwa, Dr. Yuko Shimada-Niwa, Ms. Reiko Kise, Dr. Outa Uryu, Mr. Tomotsune Ameku, Mr. Tatsuya Komura, Mr. Yota Hirano, Ms. Kana Morohashi, Mr. Eisuke Imura, Mr. Yu Takao, Ms. Hitomi Takemata, Ms. Chikana Yamamoto, Dr. Kazumasa Hada, Dr. Maki Kashikawa-Yoshida, and Dr. Takuji Yoshiyama-Yanagawa for helping, advising, and teaching me.

I thank Dr. Fumihiko Igarashi, Dr. Masatoshi Iga, Dr. Hiroshi Kataoka, and Dr. Tetsuro Shinoda for collaborating with me.

I thank Dr. Ryusuke Niwa, Dr. Kazuto Nakada, Dr. Yasunori Sasakura and Dr. Katsuo Tokunaga-Furukubo for my Thesis Advisory Committee to.

I thank Dr. Takashi Matsuo, Dr. Michael B. O'Connor, Dr. Satomi Takeo, and Dr. Jeongbin Yim for advising me on technical points and generously providing materials.

I thank Dr. François Payre and Dr Yuji Kageyama for discussing unpublished data about *nobo/GSTe14*.

I thank the Bloomington Drosophila Stock Center, the Drosophila Genetic Resource

Center in Kyoto, the Vienna Drosophila RNAi Center, and the Developmental Studies Hybridoma Bank for providing *Drosophila* strains and reagents.

Supplemental table

GST proteins used for phylogenetic analysis in Figure 9. Red characters indicate Nobo sub-family GSTs.

Species	Gene ID	Cluster
Aedes aegypti	AAEL000092	GSTx1
	AAEL004229	GSTt4
	AAEL001054	GSTd4
	AAEL001059	GSTd3
	AAEL001071	GSTd5
	AAEL001078	GSTd2
	AAEL001061	GSTd1
	AAEL001090	GSTd7
	AAEL006764	Delta-GST
	AAEL007955	GSTe8
	AAEL007954	GSTe1
	AAEL007962	GSTe4
	AAEL007951	GSTe2
	AAEL007964	GSTe5
	AAEL007948	GSTe7
	AAEL007946	GSTe6
	AAEL007947	GSTe3
	AAEL009020	GSTt3
	AAEL009017	GSTt1
	AAEL009016	GSTt2
	AAEL009602	
	AAEL010500	GSTx2
	AAEL010582	GSTd11
	AAEL010591	GSTd6
	AAEL011741	GSTs1
	AAEL011752	GSTi1
	AAEL011934	GSTz1
	AAEL015336	GST
	AAEL017085	GSTo1
Anopheles gambiae	AGAP005749	GSTO1
	AGAP006132	GST

	AGAP002898	GSTZ1
	AGAP003257	GSTU2
	AGAP004163-PB	GSTD7
	AGAP004164-PC	GSTD1
	AGAP004165	GSTD2
	AGAP004171	GSTD8
	AGAP004172	Delta-GST
	AGAP004173	GSTD5
	AGAP004378	GSTD11
	AGAP004379	GSTD6
	AGAP004380	GSTD12
	AGAP004381	GSTD4
	AGAP004382	GSTD3
	AGAP004383	GSTD10
	AGAP010404	GSTS1
	AGAP009190	GSTE8/U4
	AGAP009191	GSTE6
	AGAP009192	GSTE5
	AGAP009193	GSTE4
	AGAP009194	GSTE2
	AGAP009195	GSTE1
	AGAP009196	GSTE7
	AGAP009197	GSTE3
	AGAP009342	GSTU3
	AGAP000761	GSTT1
	AGAP000888	GSTT2
	AGAP000947	GSTU1
	AGAP012702	Delta-GST
	AGAP012838	Delta-GST
	AGAP012839	Partial;Delta-GST
Tribolium castaneum	Tc_04450	Epsilon-GST
	Tc_04449	Epsilon-GST
	Tc_04448	Epsilon-GST
	Tc_04447	Epsilon-GST
	Tc_04940	Epsilon-GST

	Tc_04941	Epsilon-GST
	Tc_04942	Epsilon-GST
	Tc_04446	Epsilon-GST
	Tc_04445	Epsilon-GST
	Tc_04444	Epsilon-GST
	Tc_04443	Epsilon-GST
	Tc_04442	Epsilon-GST
	Tc_00522	Theta-GST excluded
	Tc_03231	Sigma-GST
	Tc_03232	Sigma-GST
	Tc_03233	Sigma-GST
	Tc_03336	N-terminal domain only
	Tc_03104	Partial; Epsilon-GST
	Tc_03345	Epsilon-GST
	Tc_03346	Epsilon-GST
	Tc_03347	Partial; Epsilon-GST
	Tc_03348	Epsilon-GST
	Tc_03103	Epsilon-GST
	Tc_03496	Sigma-GST
	Tc_02878	Sigma-GST
	Tc_00067	Sigma-GST
	Tc_00055	Omega-GST
	Tc_00054	Omega-GST
	Tc_03873	Omega-GST
	Tc_07571	Delta-GST
	Tc_09482	Epsilon-GST
	Tc_09842	Zeta-GST
	Tc_06215	Theta-GST
Culex quinquefasciatus	CPIJ000031	Omega-GST
	CPIJ006159	Sigma-GST
	CPIJ006160	Sigma-GST
	CPIJ018624	Epsilon-GST
	CPIJ018625	Epsilon-GST
	CPIJ018626	Epsilon-GST

	CPIJ018627	Epsilon-GST
	CPIJ018628	Partial; Epsilon-GST
	CPIJ018629	Epsilon-GST
	CPIJ018630	Epsilon-GST
	CPIJ018631	Epsilon-GST
	CPIJ018632	Epsilon-GST
	CPIJ018633	Epsilon-GST
	CPIJ019572	Theta-GST
	CPIJ000304	Delta-GST
	CPIJ009434	Delta-GST
	CPIJ009240	GST
	CPIJ020053	Theta-GST
	CPIJ010814	Partial; Delta-GST clusters with CPIJ002680
	CPIJ002660	Delta-GST
	CPIJ002661	Delta-GST
	CPIJ002663	Delta-GST
	CPIJ002674	Delta-GST
	CPIJ002675	Delta-GST
	CPIJ002676	Delta-GST
	CPIJ002677	C-terminal domain only
	CPIJ002678	Delta-GST
	CPIJ002679	Delta-GST
	CPIJ002680	Delta-GST
	CPIJ002681	Delta-GST
	CPIJ002682	Partial; Delta-GST
	CPIJ002683	Delta-GST
	CPIJ014051	Theta-GST
	CPIJ014052	Theta-GST
	CPIJ014053	Theta-GST
	CPIJ014054	Theta-GST
	CPIJ014694	Delta-GST
	CPIJ016212	Delta-GST
	TBLASTN	Cp_GSTZ; overlaps with CPIJ009709
Drosophila	FBpp0087660	Epsilon-GST

melanogaster		
	FBpp0087548	Theta-GST
	FBpp0087549	Theta-GST
	FBpp0086857	Epsilon-GST
	FBpp0086157	GSTS1
	FBpp0085905	GSTE10
	FBpp0085850	GSTE1
	FBpp0085851	GSTE2
	FBpp0085852	GSTE3
	FBpp0085853	GSTE4
	FBpp0085854	GSTE5
	FBpp0085855	GSTE6
	FBpp0085856	GSTE7
	FBpp0085857	GSTE8
	FBpp0085858	GSTE9
	FBpp0085876	Epsilon-GST
	FBpp0072341	Epsilon-GST
	FBpp0076348	Omega-GST
	FBpp0076349	se;Omega
	FBpp0076378	Omega
	FBpp0076376	Omega-GST
	FBpp0113023	gfzf;Delta/Epsilon superclass2
	FBpp0081522	Zeta-GST
	FBpp0081520	Zeta-GST
	FBpp0082079	GSTD10
	FBpp0082078	GSTD9
	FBpp0082077	GSTD1
	FBpp0082041	GSTD2
	FBpp0082042	GSTD3
	FBpp0082043	GSTD4
	FBpp0082044	GSTD5
	FBpp0082045	GSTD6
	FBpp0082046	GSTD7
	FBpp0082047	GSTD8
	FBpp0113057	Delta-GST

	FBpp0073609	Theta-GST
	FBpp0077002	Theta-GST
Bombyx mori	BGIBMGA002222	GSTd2
	BGIBMGA002211	GSTd3
	BGIBMGA002279	GSTe2
	BGIBMGA005064	GSTz1
	BGIBMGA006537	GSTd1
	BGIBMGA006538	Delta-GST
	BGIBMGA006639	Partial(C-terminal domain only)
	BGIBMGA007860	Partial;divergent;GSTz2
	BGIBMGA009106	GSTs1
	BGIBMGA009107	GSTs2
	BGIBMGA009607	Partial;GSTo3;condirmed by SilkDB
	BGIBMGA009935	GSTt1
	BGIBMGA009951	GSTe3
	BGIBMGA010094	GSTe4
	BGIBMGA010093	GSTe5
	BGIBMGA011658	GSTo2
	BGIBMGA011819	GSTo1
	BGIBMGA011820	GSTo4
	BmGSTe7	BmGSTe7
Pediculus humanus	PHUM009630	Sigma-GST
	PHUM097960	Partial;Delta-GST
	PHUM189430	Delta-GST
	PHUM189440	Delta-GST
	PHUM236630	
	PHUM284550	Sigma-GST
	PHUM284560	Partial;Sigma-GST
	PHUM284770	Sigma-GST
	PHUM333090	Delta-GST
	PHUM454040	Theta-GST
	PHUM530530	Omega-GST
Nasonia vitripennis	XP_001605303	GSTT2
	XP_001608225	GSTS1
	XP_001607824	Partial;GSTS22;Clusters;with S3,S8,S1

	XP_001608207	GSTD5
	XP_001599411	GSTS3
	XP_001603942	GSTS4
	XP_001605098	Partial;GSTS61
	XP_001605456	GSTS5
	XP_001600473	GSTS7
	XP_001600977	GSTS8
	XP_001600187	GSTD4
	XP_001600762	GSTO1
	XP_001601032	GSTO2
	XP_001606174	GSTD3
	XP_001607855	GSTD1
	XP_001603686	GSTT1
	XP_001603714	GSTT3
	TBLASTN	GSTZ1
Apis mellifera	GB11466	GSTO1
	GB14372	GSTS4
	GB17672	GSTZ1
	GB18045	GSTD1
	GB30268	Partial;GSTS21
	GB16959	GSTS1
	GB10031	GST
	GB19678	Partial
	GB12047	GSTT1
Acyrthosiphon pisum	ACYPI002127	Sigma-GST
	ACYPI002679	Sigma-GST
	ACYPI000794	Sigma-GST
	ACYPI009586	Delta-GST
	ACYPI009122	Theta-GST
	ACYPI007233	Theta-GST
	ACYPI008340	Omega-GST
	ACYPI008042	Delta-GST
	ACYPI009519	Sigma-GST
	ACYPI008550	Delta-GST
	ACYPI009326	Sigma-GST

	ACYPI52132	Partial
	ACYPI001068	Delta-GST
	ACYPI008657	Delta-GST
	ACYPI006899	Delta-GST
	ACYPI52302	Delta-GST
	ACYPI005620	Delta-GST
Danaus plexippus	DPGLEAN14383	GSTE3
	DPGLEAN07422	GST-containing FLYWCH zinc-finger protein, isoform B
	DPGLEAN00802	GSTD1
	DPGLEAN00407	CG16936
	DPGLEAN04701	CG9363-A
	DPGLEAN15774	CG6776
	DPGLEAN17330	GSTE4
	DPGLEAN10649	GSTE7
	DPGLEAN10896	suppressor of ref(2)P sterility
	DPGLEAN09486	GSTE7
	DPGLEAN12507	GSTD1-A
	DPGLEAN06785	GSTS1-C
	DPGLEAN06787	GSTS1-C
	DPGLEAN13104	GSTE7
	DPGLEAN21737	failed axon connections, isoform C
	DPGLEAN03237	CG6776
	DPGLEAN03240	CG6776
	DPGLEAN19980	chloride intracellular channel
	DPGLEAN02728	CG4623
	DPGLEAN04969	CG9362
	DPGLEAN02611	GSTS1-C
	DPGLEAN04127	CG9393
	DPGLEAN02423	CG1702-B
	DPGLEAN01745	GSTS1-C
	DPGLEAN01768	CG17639-A
	DPGLEAN14398	GSTE1
Caenorhabditis elegans	CeGST43	

	CeGST42	
	CeY53G8B1	
	CeY53F4B33	
	CeY53F4B29	
Homo sapience	HsGSTA3	
	HsGSTA2	
	HsGSTA1	